8-2014

Finite Element Analysis of Structural Acoustic Interaction with Air and Water for Sound Transmission Through Honeycomb and Double Walled Panels with Air Cavity

Amit Shivaraj Bendigeri
Clemson University, abendig@clemson.edu

FINITE ELEMENT ANALYSIS OF STRUCTURAL ACOUSTIC INTERACTION WITH AIR AND WATER FOR SOUND TRANSMISSION THROUGH HONEYCOMB AND DOUBLE WALLED PANELS WITH AIR CAVITY

A Thesis
Presented to
the Graduate School of
Clemson University

In Partial Fulfillment
of the Requirements for the Degree
Master of Science
Mechanical Engineering

---

by
Amit S. Bendigeri
May 2014

Accepted by:
Dr. Lonny L. Thompson, Committee Chair
Dr. Gang Li
Dr. Huijuan Zhao

ABSTRACT

A measure of Sound Transmission Loss (STL) through panel structures is the ratio of the average power over the panel surface from an incident acoustic pressure wave interacting with the surface of one side of the panel with the transmitted average power on the other side of the panel. For panels filled with an air cavity defined by a depth between the two panels, the panel interacting with the incident acoustic wave vibrates producing structure-born sound to radiate through the cavity and interacts with the transmitted side panel, causing sound to radiate into the acoustic region on the transmitted side. For steady-state frequency response analysis, power is measured from the integration across the panel surface of the product of acoustic pressure and velocity component normal to the surface. In contrast to water coupling, the effect of air on the structural vibration response is relatively small. For air, since the acoustic impedance defined as the ratio of pressure to velocity is constant and given by the product of mass density for air multiplied by the speed of sound, the expression for STL is simplified as the ratio of incident to transmitted pressure amplitude.

In the present work, a finite element model for prediction of sound power transmission through single panel, air cavity filled double panel structures, lattice panel structures, and honeycomb panels is presented. In the case a double-panel with internal air cavity model, parameter studies are conducted to compare STL results with different cavity depths in relationship to acoustic wavelengths. Results show that STL is reduced when the wavelength is twice the depth, implying that a strong transmission effect is present

associated with the fundamental resonance cavity frequency with zero vibration nodes in the depth direction. Comparisons between single panel, Air-filled Double and Triple Panel structures are studied. As the number of panel layers is increased the thickness of each panel is decreased to have the same total mass. Air-cavity interactions in layered panels play an important role in sound transmission. Results show that more layers of thinner panels have stronger Air-cavity interactions showing stronger Air-cavity resonances in the frequency response for STL. Overall, multilayered panels with the same total mass show increased STL over the range of frequencies studied between 0 and 2000 Hz.

Further studies are conducted to study the effect of connecting the panels with periodic lattice structures. By connecting the panels, the STL is reduced, while significantly increasing the stiffness and strength under other mechanical loads. Air-cavity effects in panels with periodic connections between the panels, while introducing cavity resonances in the structure frequency response, does not significantly alter the Structure-borne sound radiation and overall STL characteristics. This study helps in understanding the challenges in designing structures needed to exhibit good structural rigidity and also has good sound insulation.

Honeycomb sandwich panels exhibit desirable structural properties of high stiffness and low mass. Previous studies have examined the STL characteristics for honeycomb panels interacting with air, up to 1000 Hz and showed that in this frequency range, Auxetic honeycomb with the total mass, which exhibit a negative effective Poisson ratio, gives

higher STL compared to Regular honeycomb. In the present work, it is shown that for frequencies between 1000 Hz and 1600 Hz, the STL for Auxetic is reduced below the STL value for Regular honeycomb. Beyond 1600 Hz, the STL for Regular honeycomb is significantly reduced.

Previously studies have not considered the interaction of water with honeycomb panels. In this work, the STL characteristics for the honeycomb panels with water on both sides, and mixed combinations of Air on Incident side and Water on transmitted side and Water on Incident side and Air on transmitted side are given. In the case of water on both sides of the honeycomb panels, the overall STL is significantly reduced compared to air interaction on both sides, and over the entire range up to 2000 Hz, Auxetic exhibited higher STL compared to Regular. In mix-match cases of Air-Water and Water-Air, Regular exhibited higher STL over Auxetic.

In addition to the steady-state analysis discussed above, a transient analysis of acoustic plane interaction waves propagating and interacting with panels are also discussed and correlations are made with the results of time-harmonic procedures. Two plane interaction waves are considered, sinusoidal amplitude driven at 100 Hz, and modified Ricker pulse amplitudes spread over a broader range of frequency but centered at 100 Hz.

DEDICATION

This thesis is dedicated to my parents Mr. Shivaraj V. Bendigeri and Mrs. Lata S. Bendigeri and my sister Ms. Shilpa S. Bendigeri. Their love and support has helped me achieve success throughout my graduate studies.

ACKNOWLEDGEMENT

I would like to thank my advisory committee chair, Dr. Lonny L. Thompson for his invaluable inputs and support in my graduate studies at Clemson University. His feedback has helped me achieve immense success in research. I would like to thank my committee members Dr. Gang Li and Dr. Huijuan Zhao, for their help and support in this research.

I would like to thank all the members of Innovative Computational Engineering and Mechanics Laboratory for their advice and support.

TABLE OF CONTENTS

Page

Table of Contents (Continued)

Page

Table of Contents (Continued)

Page

Table of Contents (Continued)

Page

Table of Contents (Continued)

Page

Table of Contents (Continued)

Page

LIST OF TABLES

Table Page

LIST OF FIGURES

Figure Page

List of Figures (Continued)

Figure Page

List of Figures (Continued)

Figure Page

List of Figures (Continued)

Figure Page

List of Figures (Continued)

Figure Page

List of Figures (Continued)

Figure Page

CHAPTER 1: MOTIVATION AND BACKGROUND

Sound transmission through panels used to partition rooms and spaces are of great interest for sound insulation applications. Of particular interest are double panels containing air cavities [1-3]. Analysis of infinite double panels with finite size studs to stiffen the structure while at the same time providing good sound transmission loss (STL) has been conducted by Lin and Garrelick [4]. In [4], the sound transmission characteristics of connected panels with and without acoustic-cavity effects were studied and it was found that air-borne sound due to air-cavities resonances had a minor impact on the overall sound transmission effects. Studies have developed theoretical modelling of smeared modeling of double panels connected with uniformly distributed studs with springs are compared with periodic models of double panels with lumped masses connecting them [5]. Theoretical STL values were compared with experimental test results. STL is the ratio of the average power over the panel surface from an incident acoustic pressure wave interacting with the surface of one side of the panel with the transmitted average power on the other side of the panel. For panels filled with an air cavity defined by a depth between the two panels, the panel interacting with the incident acoustic wave vibrates producing, structure-borne sound to radiate through the cavity and interacts with the transmitted side panel, causing sound to radiate into the acoustic region on the transmitted side. For steady-state frequency response analysis, power is measured from the integration across the panel surface of the product of an acoustic pressure and velocity component normal to the surface. For air, the acoustic impedance defined as the

ratio of pressure to velocity is constant and given by the product of mass density for air multiplied by the speed of sound. Thus in the case of air, the expression for STL is simplified as the ratio of incident to transmitted pressure amplitude. A prediction model developed to determine airborne sound including the effects of studs was developed using spatial transform technique [6].

In recent studies, the sound transmission properties of sandwich panels which a structural core sandwiched between double panel face sheets have been investigated in great detail. Cellular sandwich panels such as honeycomb core and other lattice structures are of particular interest due to their high strength, stiffness and low mass properties [7]. In Honeycomb sandwich panels, sound transmission losses can be significant due to the interaction of cellular core structural vibrations and the connected face sheet panels interacting with acoustic regions. Since the cellular cores have small air cavities, and the air light relative to the stiffness and mass of the cellular structures, the air cavity resonance interaction on the structural vibration for low to medium frequencies (longer wavelengths are usually neglected). Hence previous studies [8-10] have neglected the need for considering the acoustic properties of the acoustic cavities in between the honeycomb cores. In this study we are interested in finding whether there are any significant differences in the Sound transmission characteristics of the sandwich panels with honeycomb core when including internal acoustic air cavity interactions. As defined earlier the sound insulation in a material is most commonly known as sound transmission loss (STL) [7, 11]. Honeycomb sandwich panels have been widely used in wide array of

applications for their desirable properties of low mass and high stiffness. Honeycomb sandwich panels are used for varied effective mechanical properties achieved through changing the core geometries. Many studies have examined the STL characteristics by varying the core geometries and found that sandwich panels performed better compared to single panels. Recently general mechanical and core geometric properties of honeycomb sandwich panels have been studied by [8, 12, and 13]. STL in Regular and Auxetic honeycomb panels was studied by varying the unit cell angles and Auxetic model was found to have higher STL than Regular model [10] for the panels studied up to 1000 Hz. Regular honeycomb is characterized by hexagonal periodic unit cells with equal side lengths and angles. The effective stiffness properties are orthogonal with a Poisson's ratio of 1. For auxetic hexagonal honeycomb unit cells, the geometry has alternating interior angles and produces an effective negative Poisson's ratio. A negative Poisson's ratio is not found in naturally occurring materials and has interesting possibilities for novel design. In [9], a multi-objective procedure was designed to vary the core geometries in order to maximize STL for frequency ranges of 200 Hz to 400 Hz. All published studies have concentrated on Honeycomb sandwich panels with Air as the external acoustic domain interacting with both regular and auxetic unit cell geometries.

In fluid-structure interaction problems, the interaction between a water and structure significantly affects the response of the structure. These interactions need to properly account for the resonant properties of the acoustic fluid. The mass of water is 1000 times larger than air and has a significant coupling effect with the thin-walled elastic panel

structures studies. This fluid-structure interaction requires a fully coupled structural-acoustic solution and the vibration, fluid loading, and structural-born acoustic radiation and sound transmission loss are expected to be significantly different than for air. In the present work, we study various configurations in order to study these interaction properties. In addition to the external air or water interaction with the panels, Honeycomb sandwich panels are modelled with and without air in its cavities, to study its effects on acoustic response of the structure.

1.1 Structure-fluid acoustic characteristics

For the analysis of a sound transmission through double panel and honeycomb sandwich panels, a 2D model is assumed with the third dimension taken as infinite. Thus all excitation and response is assumed in a 2D plane, with unit depth in the third dimension. Using this approach the panel and honeycomb structures can be modeled as beams with cross-section of 1 meter in the third dimension. It is thus of interest to identify the wave properties for elastic beam structures. For this study, a beam of thickness 't' of 0.006848 meters and length 'L' of 2 meters. The beam has material properties of Aluminum of young's modulus $71.9*10^9$ GPa and a poisson's ratio of 0.3 and mass density in ρ_{air} of 2700 kg/m3. Acoustic fluid domain has Air properties as a reference with bulk modulus of 'K' of 141179 N/m^2 and density 'ρ_{air}' of 1.2 kg/m^3 is studied.

1.1.1 Waveform types

In the analysis of sound transmission in structures with acoustic interactions, two types of waves are generated, namely Structure-borne sound due to vibrations and normal velocity

components on the interacting surface, and fluid-borne sound due to propagation and resonance in internal cavities. Structure borne sound is of major significance in solving noise related problems.

For the analysis of sound transmission through double panel and honeycomb sandwich panels, a 2D model is assumed with the third dimension taken as infinite. Thus all excitation and response is assumed in a 2D plane, with unit depth in the third dimension. Using this approach the panel and honeycomb structures can be modeled as beams with cross-section of 1 meter in the third dimension. It is thus of interest to identify the wave properties for elastic beam structures.

In elastic beam structures defined by cross-section dimensions smaller than the length dimensions, various types of waves are responsible for vibrations in finite sized beams resulting in sound generation. Wave types where displacement is normal to the beam axis and therefore also normal to the propagation direction of wave is called a Bending wave. Torsional waves are created when there are torsional forces acting on a beam depending on the beam orientation in a 3-dimensional space. Longitudinal waves are created when displacement is along the beam axis. Structural bending waves are efficient at generating structural-born sound.

1.1.2 Bending waves in beams:

The following equation represents bending waves in a thin beam modeled with classical Bernoulli-Euler theory [11, 14]:

$$\rho A\ddot{\xi} + EI\frac{\partial^4 \xi}{\partial x^4} = F' \tag{1.1}$$

where, ρ is density of beam in kg/m^3 and A is the cross sectional area of the beam, $\ddot{\xi}$ is the second time derivative of displacement of the beam in transverse direction. E and I are young's Modulus and Area moment of inertia respectively. F' is the external transverse force per unit length of the beam. Bernoulli-Euler beam theory includes rotational deformation of the cross-section due to bending, but neglects transverse shear deformation. Plane sections are assumed straight and normal after deformation. In this model, the cross-section rotation due to bending deformation is assumed equal to the slope of the deflection curve defined at the centroidal axis of the cross-section.

For time-harmonic excitation, with steady-state time dependence of the form $\exp(i\omega t)$, the variables are interpreted as complex amplitudes for which the bending wave equation becomes

$$\frac{\partial^4 \xi}{\partial x^4} - \frac{\rho A}{EI}\omega^2 \xi = \frac{F'}{EI} \tag{1.2}$$

where ω is angular velocity.

1.1.3 Propagation of bending waves:

Solutions for propagating waves are characterized by the

bending wavenumber is defined by [12,14]

$$k_B = \sqrt{\omega}\left(\frac{\rho A}{EI}\right)^{\frac{1}{4}} \tag{1.3}$$

where ω is angular frequency.

Figure 1-1 plots the bending wave number over the range of frequencies in this study from 0 to 2000 Hz. It is noted that the flexural (bending) wavenumber is a nonlinear function of frequency with a non-constant slope. For reference, the wavenumber for an acoustic medium defined by $k = \frac{\omega}{c_o}$ where c_o is the speed of sound in air is shown for comparison. The acoustic wave number varies linearly with frequency with constant slope.

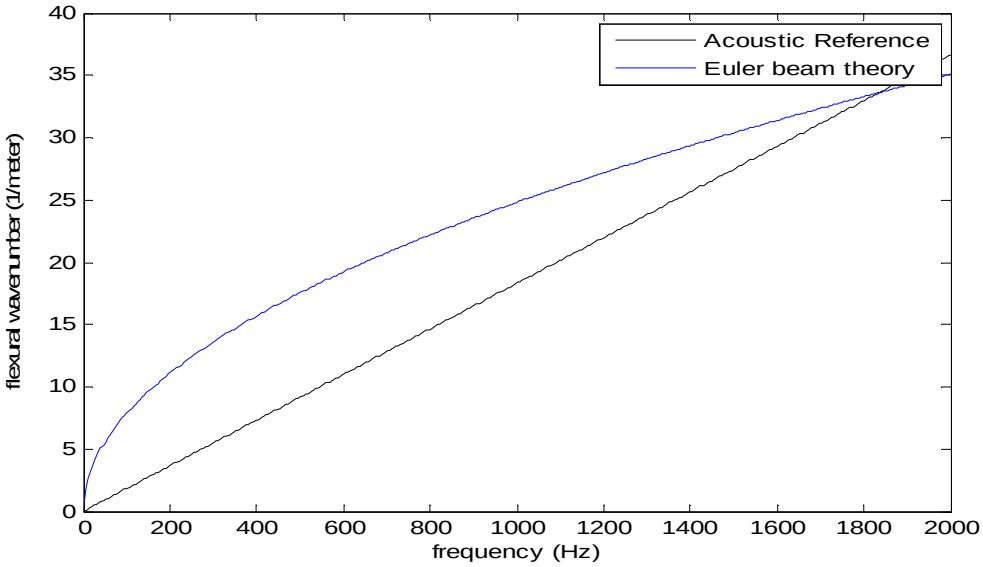

Figure 1-1 Plot of flexural wavenumber vs. frequency for the beam compared to acoustic wavenumber for air

The wavenumber can also be related to the spatial wavelength by

$$k_B = \frac{2\pi}{\lambda_B} = \frac{\omega}{c_B} \tag{1.4}$$

where λ_B the bending is wave length and c_B is bending wave speed

Substituting (1.3) in (1.4), we can express the bending wavelength (Flexural wave length) in terms on frequency

$$\lambda_B = \frac{2\pi}{\sqrt{\omega}} \sqrt[4]{\frac{EI}{\rho A}} \tag{1.5}$$

It can be observed that bending wave length λ_B in beams varies by square root of range of frequencies. For higher frequencies, the wavelength is decreased.

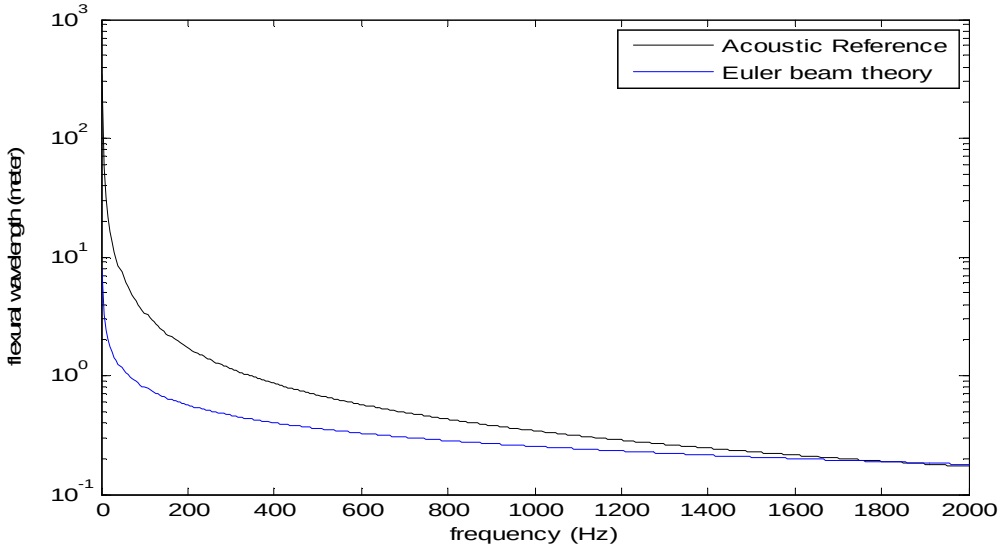

Figure 1-2 Plots of flexural wavelength vs frequency for a beam and acoustic wavelength in air for reference

Figure 1-2 plots the bending wavelength of a beam vs frequency.

The bending wave speed is defined by

$$c_B = \sqrt[4]{\frac{EI}{\rho A}}\sqrt{\omega} \tag{1.6}$$

The bending wave speed (phase velocity) is a frequency dependent parameter unlike the constant acoustic wave speed for air or water. These characteristics form the fundamental differences in differentiating bending waves in beams to air-borne and water-born waves. Figure 1-3 represents the bending wave speed vs frequency compared to the constant acoustic wave speed (speed of sound) in air of 343 m/sec.

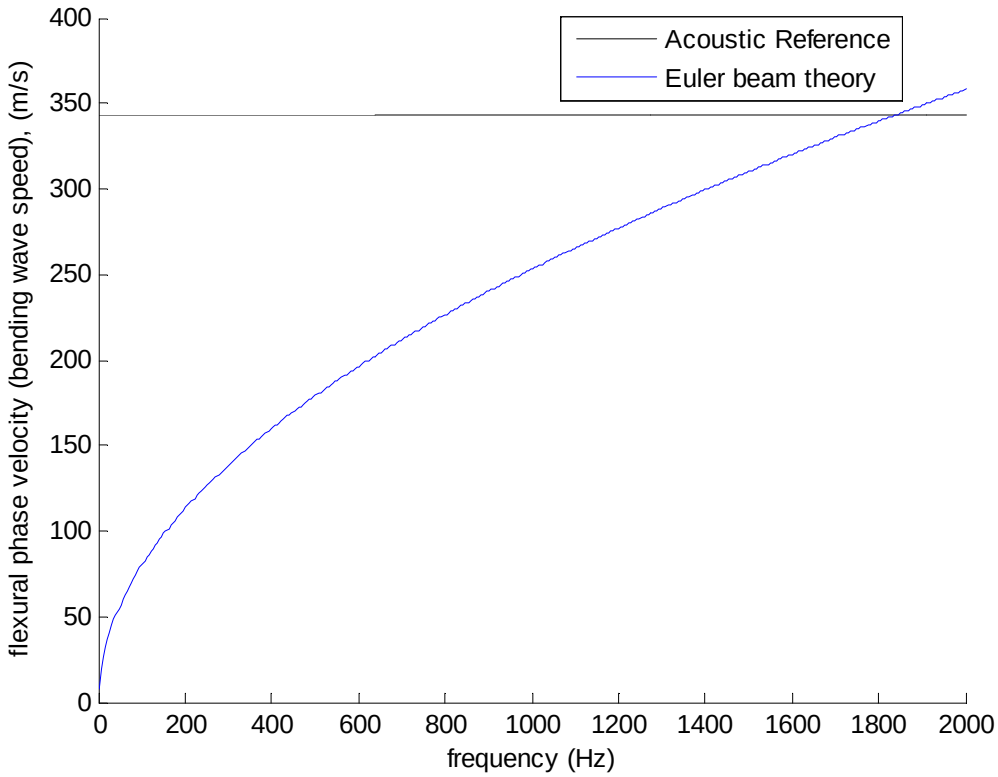

Figure 1-3 Plots for flexural phase velocity vs frequency of a beam and acoustic wave speed in air for reference

The equations for the natural resonance frequencies of mode shapes for a simply supported beam of length L, based on classical Bernoulli-Euler beam theory is given by

$$f_{mode} = \frac{1}{2\pi} k_n{}^2 \sqrt{\frac{EI}{\rho A}}, \text{ where } k_n = \frac{n\pi}{L} \tag{1.7}$$

Figure 1-4 below plots the theoretical bending natural frequencies vs. mode numbers up to the first 20 modes for a finite length of L=2m.

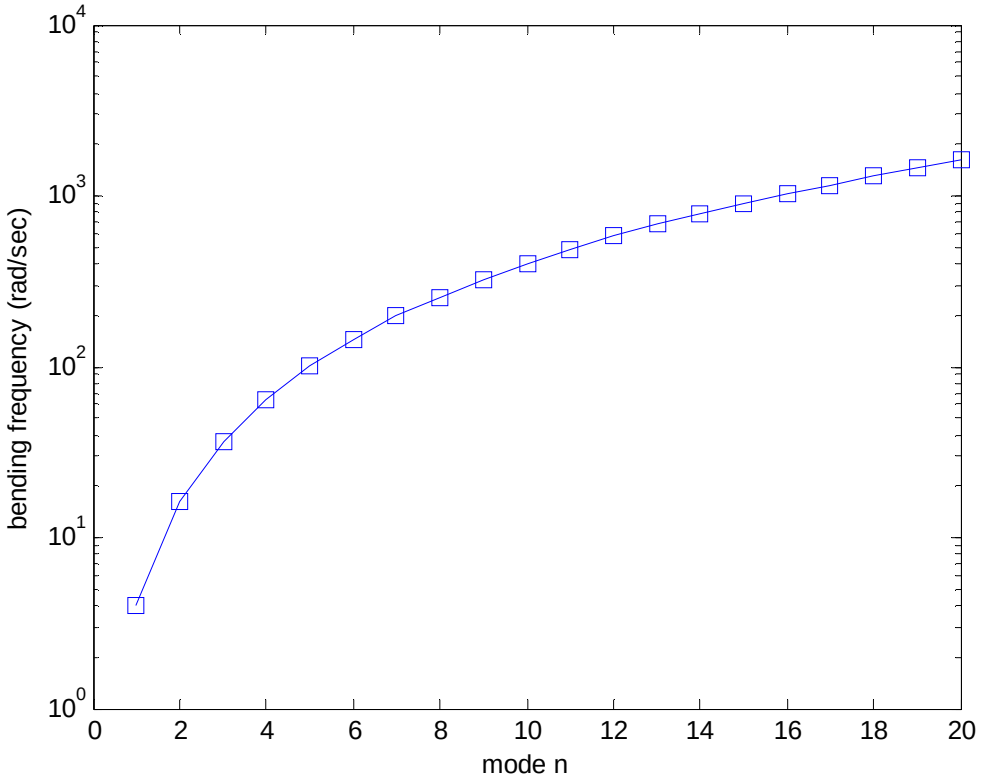

Figure 1-4 Bending frequency vs mode for a finite simply-supported beam

In the case of time-dependent transient analysis, with excitation from a pulse function with Fourier transform consisting of a range of frequency components, the frequency dependent bending wave speed causes these spectral components to ‘run away from each other, the larger is the distance between frequencies. This means that the spectral composition is different for the beam at two different locations and has two different time characteristics of beam velocities. Hence distortions in time signal are encountered along the propagation direction of the bending wave[14]. The effect is called dispersion.

1.1.4 Propagation of waves in air:

As discussed earlier, there are fundamental differences in the propagation properties of acoustic waves in a medium such as air or water in comparison to elastic waves in beam structures. An important aspect is that the wave speed (phase velocity), also called the speed of sound, in air or water is constant irrespective of the frequency of study is given as

$$c_0 = \sqrt{\frac{K}{\rho}} \tag{1.8}$$

where K is the bulk-modulus for air or water and ρ_f is the mass density for air or water. The spatial wave number for acoustics is

$$k_0 = \frac{\omega}{c_{air}} \tag{1.9}$$

With spatial wavelength,

$$\lambda_0 = \frac{2\pi}{k_0} \tag{1.10}$$

1.1.5 Propagation of bending waves using Timoshenko beam theory

Formulas derived earlier for propagation of bending waves neglected the transverse shear deformation and sectional rotary inertia. The following equations consider the transverse shear deformation and cross-section rotary inertia according to Timoshenko Beam theory.

In this theory, the slope of the deflection curve of the centroidal axis and the section rotation are independent parameters. Assuming time-harmonic propagating solutions in the equations for deflection of the centroidal axis and section rotation results in a quadratic polynomial for the bending wavenumber squared in terms of frequency squared: $c_1 k^4 + c_2 k^2 + c_3 = 0$. The coefficients in the quadratic equation are

$$c_1 = \left(\frac{A}{I} - \frac{\omega^2}{\left(k' c_g\right)^2} \right) \tag{1.11}$$

$$c_2 = \left(\frac{c_e^{\,2}}{\left(k' c_g\right)^2} + 1 \right) \omega^2 \tag{1.12}$$

$$c_3 = -c_e^{\,2} \omega^2 \tag{1.13}$$

where

$$c_e = \sqrt{\frac{E}{\rho}}, c_g = \sqrt{\frac{G}{\rho}} \tag{1.14}$$

and E and G are Young's modulus and shear modulus respectively for the material. Solving this quadratic polynomial for their roots finds the Timoshenko bending wave number, and hence and hence the Flexural Wavelength of the beam given as

$$\lambda_{timoshenko} = \left(\frac{2\pi}{k_{timoshenko}} \right) \tag{1.15}$$

The phase speed for bending waves based on Timoshenko theory is defined by $c_{timoshenko} = \omega / k_{timoshenko}$. The flexural wavelength for Timoshenko beam theory is plotted in Figure 1-5. For the properties considered, the Timoshenko and Euler beam theories have nearly the same wavelength

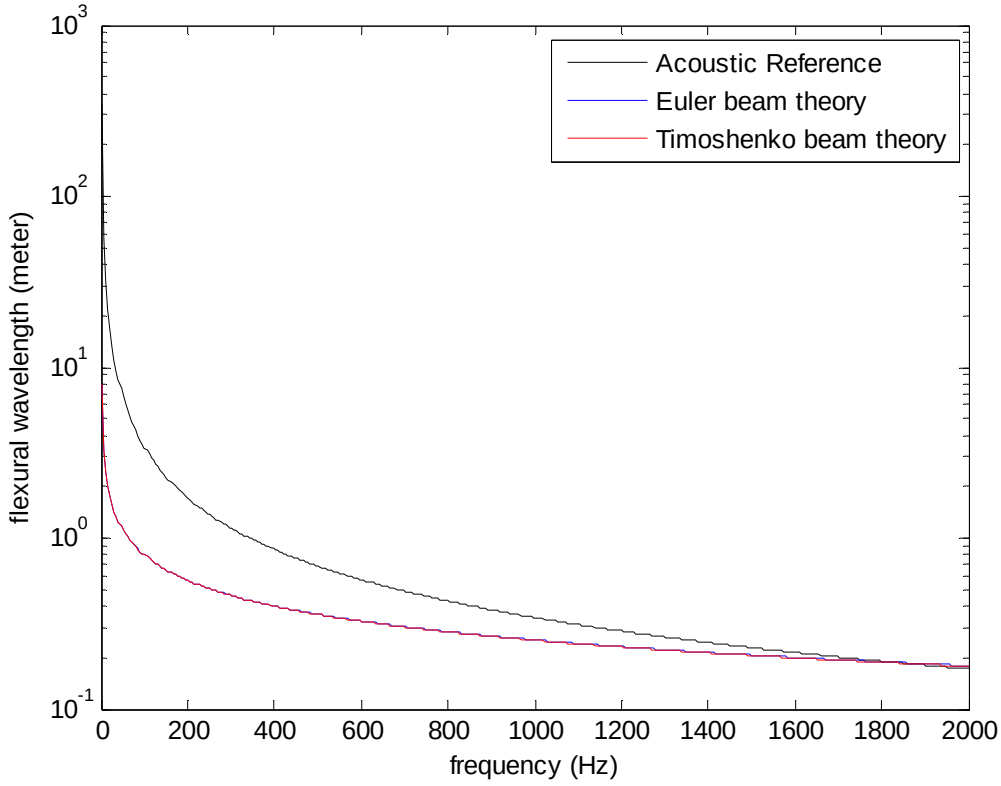

Figure 1-5 flexural wavelength vs frequency comparison for Euler and Timoshenko beam theory

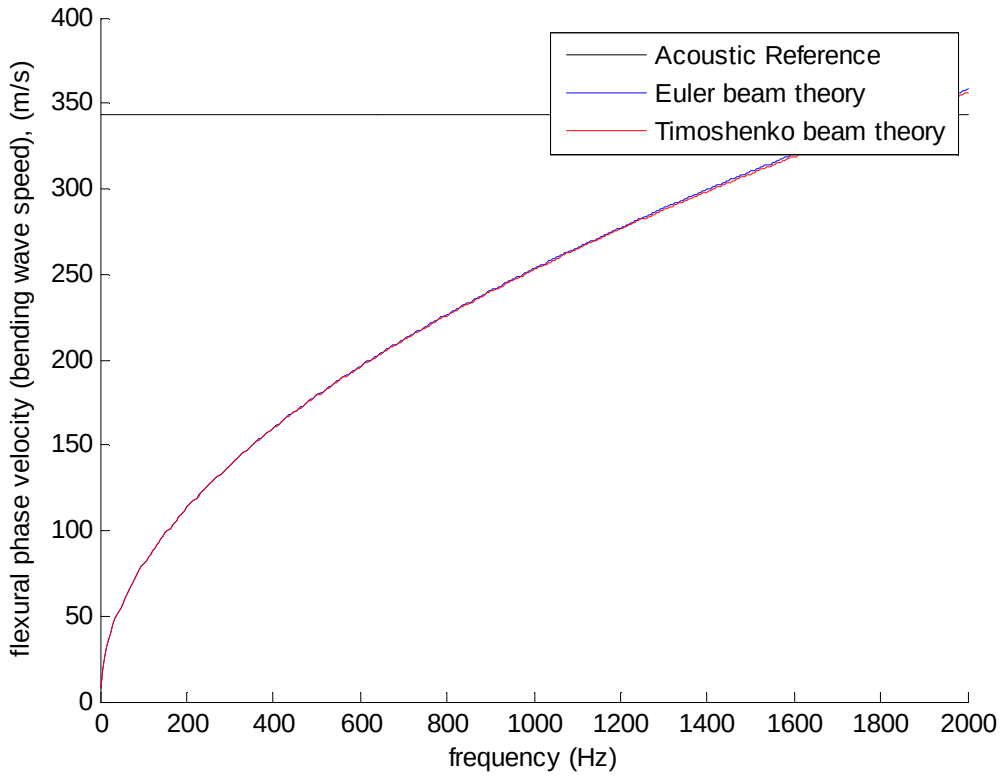

Figure 1-6 Comparison of flexural phase velocity of Euler and Timoshenko beam theory

The relationship between wave number is and phase speed for is given by

$$k_{timoshenko} = \frac{\omega}{c_{timoshenko}} \tag{1.16}$$

The phase speed is given in Figure 1-6 and the wavenumber is given in Figure 1-7. For the properties considered, Timoshenko theory matches Euler frequency for the frequency range considered up to 2000 Hz. About 1600 Hz, there are small differences observed.

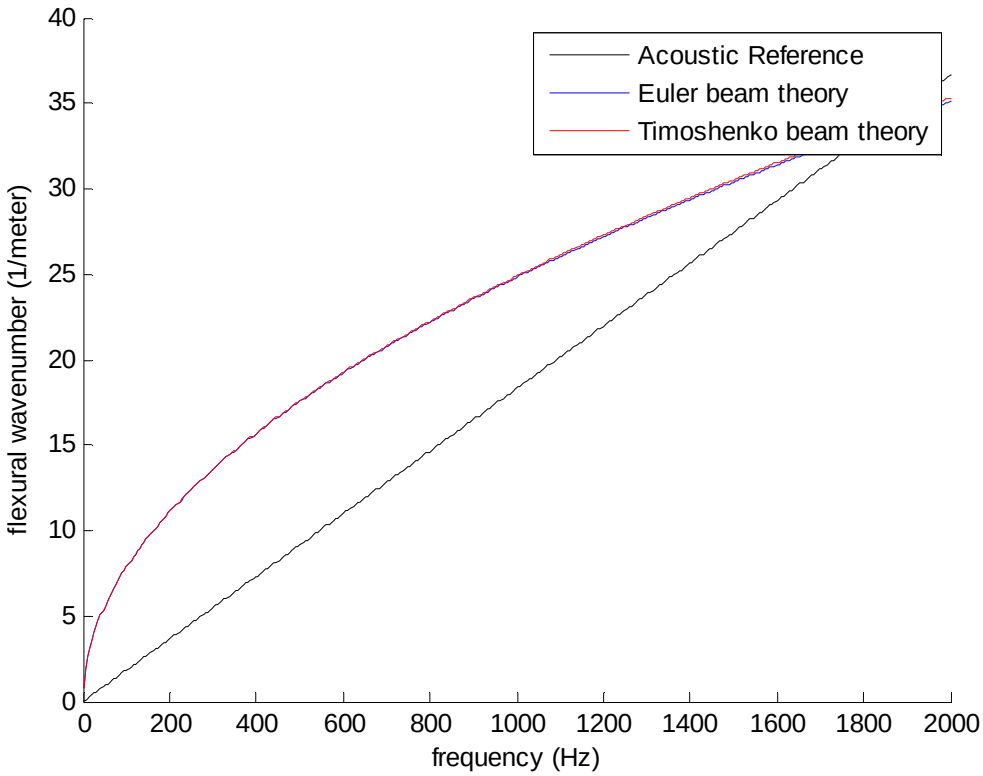

Figure 1-7 Comparison of Flexural wavenumber for Euler beam theory and Timoshenko beam theory

Thicknesses of the beam have a significant impact on the flexural wavelength and a plot showing its dependence is shown in Figure 1-8.

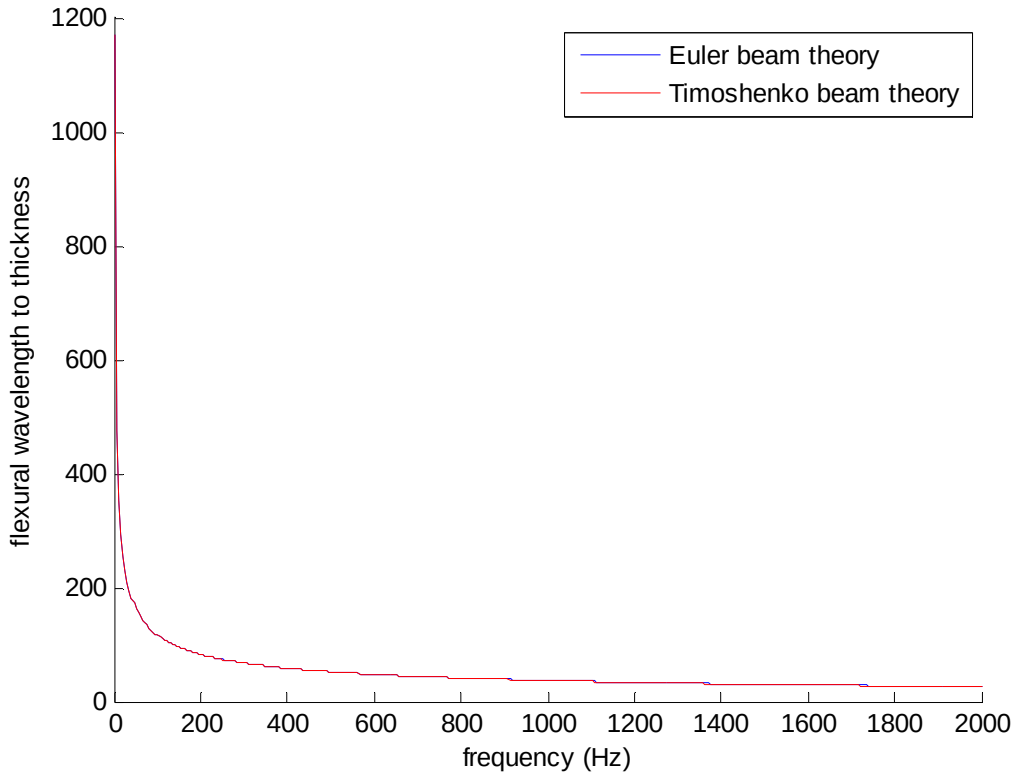

Figure 1-8 Comparison of flexural wavelength for Euler and Timoshenko beam theory

These properties presented above are significant in estimating the number of beam elements required and mesh size for adequate numerical accuracy and convergence of the finite element analysis.

1.1.6 Natural frequencies of panel and air cavity

As discussed earlier, the natural frequencies of a single panel with simple supports (deflection restrained with free rotation) modeled with classic Bernoulli-Euler beam theory is given by

$$f_{bending} = \frac{1}{2\pi}\left(\frac{\alpha}{l}\right)^2 \sqrt{\frac{EI}{\rho A}} \tag{1.17}$$

where α = 1,2,3…

Using separation variables, the resonance frequencies of rectangular air cavity with rigid walls is given by

$$f_{air} = \frac{c_{air}}{2\pi}\sqrt{\left(\frac{m\pi}{l}\right)^2 + \left(\frac{n\pi}{d}\right)^2} \tag{1.18}$$

where m and n are non-negative integers, L_x and L_y are the dimensions of the rectangular cavity, and c_o is the speed of sound in air.

1.2 Effects of symmetric and anti-symmetric modes

For double walled panels with rectangular air cavity, for frequency ranges below coincidence frequency, STL gains are higher due to cancellations of symmetric and anti-symmetric motions of the panels with respect to the incident sound field. The symmetric and anti-symmetric modes of the incident panel follow a similar phase relative to the acoustic incident wave field. However the transmitting panels have superimposed motions nearly out of phase reducing the sound transmission [14].

1.3 Objectives

As discussed earlier, Honeycomb sandwich panels exhibit desirable structural properties of high stiffness and low mass. Previous studies have examined the STL characteristics for honeycomb panels interacting with air, up to 1000 Hz and showed that in this frequency range, Auxetic honeycomb with the total mass, which exhibit a negative effective Poisson ratio, gives higher STL compared to Regular honeycomb [10]. It is of interest to study the STL for regular and auxetic for higher frequencies beyond 1000 Hz to determine if this trend carries to higher frequencies. Thus one of the objectives of this work is to study the STL for honeycomb for frequencies up to 2000 Hz. By doubling the frequency range studied, a refined mesh must be used and further computational memory and solution time is required.

Previously studies have not considered the interaction of water with honeycomb panels. In this work, the STL characteristics for the honeycomb panels with water on both sides, and mixed combinations of Air on Incident side and Water on transmitted side and Water on Incident side and Air on transmitted side are of interest. A question to be answered is whether the trends found for honeycomb in air carry over to interaction with water, where there is significant interaction and coupling modifying the vibration and structural-born sound not present in the case of acoustics in air. In order to model water on both sides, an external acoustic domain on both sides of the panel need to be modeled and the incident plane wave cannot be modeled as done previously as a uniform pressure load applied to the incident panel surface. Instead a wave interaction must be defined with

interaction on both the acoustic interface boundary and structural beam interface for the incident panel.

In addition to studies of honeycomb panels, a more fundamental understanding of sound transmission through panels is sought. To gain insights, the honeycomb core is removed and replaced by a rectangular air cavity between the two face-sheet panels. This double panel configuration does not have any structural members connecting the incident and transmitted side panels, as a result, in addition to the external acoustic regions, the internal acoustic cavity region between the two panels must be modeled to transmit waves. The incident acoustic wave interacts with the incident panel causing vibration, this vibration causes structural-borne sound to scatter back into the incident acoustic region and also into the air cavity between the panels. The sound transmitted into the air cavity interacts with the transmitted side panel causing it to vibrate and radiate sound into the transmitted size external acoustic region. In addition, a resonance in the air cavity is generated due to the reflections between the two panels. The air in the cavity acts like an additional spring stiffness between the two thin elastic panels. The depth of the air cavity and relation to the thickness of the panels plays an important role in the sound transmission characteristics. Thus it is of interest to vary the depth of the double panel cavities and observed the sound transmission loss. In the present work, a goal is to vary the panel depth and study the role of depth to wavelength ratio as the incident acoustic wave frequency varies.

The gain further insight, thin-walled elastic periodic lattice core structures will be modeled connecting the incident and transmitted panels. In this case, a structural path of vibration connects the two panels and is the main driver for transmission between the incident panel and transmitted panel. In this case, the effects of including or not including an acoustic region within the air cavities of the lattice core structure are of interest and are studied in this work.

1.3.1 Specific objectives

The specific objectives of this work are

1. Internal air-cavity interactions in double panels play an important role in sound transmission. An objective is to understand the relationship between air cavity depths on the sound transmission loss (STL) and relate the resonance modes and wavelengths associated with fundamental natural frequencies of the air cavity and elastic panels. A parametric study will be performed to determine the effects of different depths of air-cavities on STL in double panel structures.
2. Compare the STL characteristics for single, double and triple panels with air-filled cavities. Comparisons are made between Single, Double and Triple Panels with same total mass.
3. Connecting the panels with lattice core structures, increases the strength and stiffness is of the sandwich panel structure. A goal is to study the sound transmission effects of air-cavities in panels with periodic lattice cores connecting the incident side panel to the transmitted side panel. In order to maintain a

common high frequency limit for STL, the total mass for each structure consider is kept same. This is accomplished by changing the thickness of the lattice core structures and face sheet panels so that total mass is the same.

4. Previous studies have examined Honeycomb sandwich panels for their sound transmission characteristics for a frequency range up to 1000 Hz [10]. In order to study the STL characteristics for higher frequencies, the range is doubled for up to 2000 Hz.
5. Earlier studies on STL have only concentrated on Air as the exterior acoustic domain interacting with Honeycomb sandwich panels. We are interested in finding the STL characteristics for heavier fluids such as water which have stronger interactions with the sandwich panels. Thus another important goal of this work is to investigate the STL effects of Honeycomb panels with water as the acoustic domain, and mix-match conditions of air on the incident side and water on the transmitted side and vice versa.

1.4 Thesis overview

Chapter 1:

Here we introduce the concepts and theories developed earlier to study the effects of Air-cavities in double panels and panels connected by periodic connections. STL in honeycomb sandwich panels and advantages of their effective mechanical properties along with sound absorption characteristics are explained.

Sound transmission characteristics of structures and fluids are dependent on their mechanical and material properties. In this section we elaborate on the characteristic properties affecting the sound transmission characteristics. Emphasis is given on the bending wave propagation in elastic beams and rectangular air cavities and finding the fundamental resonant natural frequencies of beam and acoustic rectangular cavities. Effects of symmetric and anti-symmetric modes are also studied.

Chapter 2:

In this chapter detailed steps are shown to setup a finite element model in ABAQUS for a reference double panel. Different loading conditions applied in the study are also discussed. As a part of post processing results, details about calculating STL values for structures in different acoustic fluid domains are discussed. In the last section we discuss the theory explaining blocked wave and scattering effects as a consequence in the incidence field.

Chapter 3:

This chapter presents the results for various models setup to examine the objectives listed earlier. Detailed discussions are presented on acoustic characteristics of Air-cavities and associate their depths with acoustic properties. Comparisons are made between Single, Double and Triple panels with same total mass. Air-cavity effects in panels with periodic lattice connections are studied. Results are presented for Regular and Auxetic Honeycomb panels with different combinations of Air and Water.

Chapter 4:

In this chapter we elaborate on the conclusions that can be drawn from the finite element solutions for the different structural-acoustic models considered. Acoustic Air-cavity depths in relationship with wavelength of sound in Air are discussed. Conclusions are made on the performance of STL in Regular and Auxetic in different acoustic domains.

CHAPTER 2: ACOUSTIC FINITE ELEMENT MODEL USING ABAQUS

2.1 Double-panel with acoustic air cavity as a reference model

2.1.1 Model type

The panel structure is assumed to extend to infinity in one direction, and thus will be modeled as a 2D planar problem with unit depth in the third dimension. All load excitation, structural and acoustic response will be in the 2D plane.

2.1.2 Structural- Acoustical model

The finite element model and analysis are carried out using the ABAQUS commercially available Finite element analysis (FEA) software. To validate the models created, mesh convergence studies are performed and the results for reference cases are compared to previous studies presented in the literature [10].

The reference model shown in the Figure 2-1 Double Panel Acoustical model has two thin elastic face sheet panels separated by an interior acoustic-fluid cavity of depth “d”. The transmitted side of the double panel interacts with an external fluid as acoustic domain. The exterior acoustic region extends to infinity. The condition that sound waves radiating outwards from the vibrating panel propagate to infinity without reflection, the exterior acoustic domain is truncated by a semi-circle and modeled with a local non-reflective impedance boundary condition (NRBC). The local NRBC maintains the sparsity of the finite element equations and is of increasing accuracy the further the circular NRBC is moved from the vibrating panel [15]. The two panels are simply

supported (pin connected), and the interior acoustic cavity interacts with the two panels but is constrained on its sides by a rigid condition. The double panel structure itself is mounted in a rigid baffle. The rigid condition is modeled for the acoustic region with the normal pressure gradient set to zero representing zero structural acceleration amplitude [15].

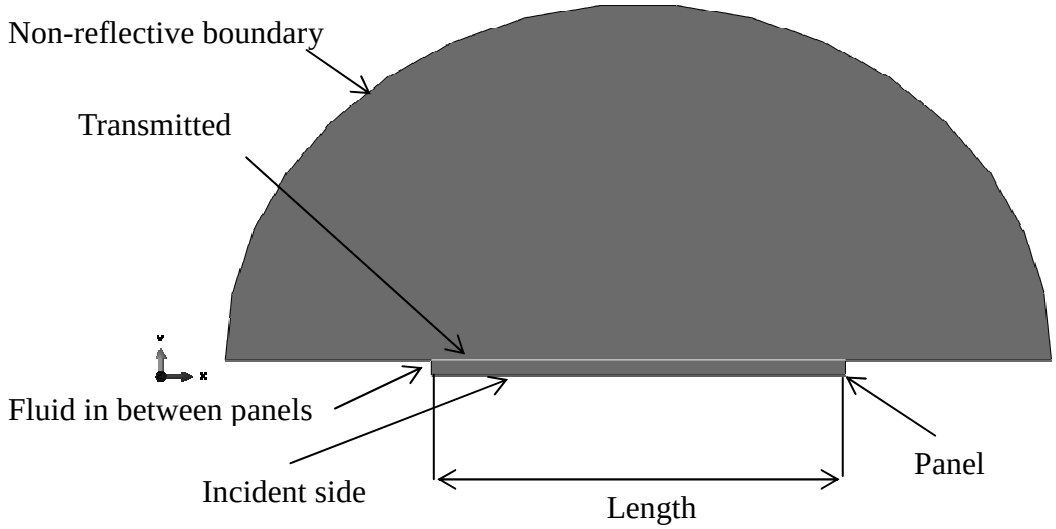

Figure 2-1 Double Panel Acoustical model

2.1.3 Parts

The 2D ABAQUS finite element model consists of two main part types. Firstly, the face sheet panels are modeled as beam elements on the principles of Timoshenko beam theory. Secondly, the acoustic fluid domains are present on the transmitted side as shown in Figure 2-1, and in between the panels in the internal acoustic cavity. However, in case

of single panel study, the fluid is only modeled on the transmitted side which is discussed later.

In terms of ABAQUS model geometry, he face sheet panels are modeled as a 2D deformable planar model with “wire profile” part. The acoustic domain is modeled as a 2D “shell” model part. The wire profile geometry is set-up for a beam element mesh, while the 2D “shell” model part is set-up to mesh with 2D acoustic elements. The length of face sheet panels are set at 2m with the depth of the acoustic region in between the face sheets is 0.0887m, which is consistent with the sandwich panel structures studied in [8-10]. The acoustic domain on the transmitted side is semi-circular and set with a 2 m radius. The out of plane thickness of the entire model is set to a unit 1 meter

2.1.4 Sections

The beam sections for the face sheet panels are assigned the out of plane dimension to have a = 1 m, with a thickness of b = t mm, where the in-plane thickness t varies according to requirements will be specified in the parameter studies.

For the 2D acoustic regions, a solid homogenous section is created.

2.1.5 Materials

The materials used in this analysis are described as follows:

Aluminum is used a standard material for face sheets with the properties described in the Table 2-1 below:

Table 2-1 Material properties of Aluminum

Mass density	Young's modulus	Poisson's ratio
2700 kg/m^3	71.9 GPa	0.3

The material properties of air are shown in Table 2-2:

Table 2-2 Material properties of Air

Mass density	Bulk modulus
1.2 kg/m^3	141179 Pa

The material properties of water are shown in Table 2-3:

Table 2-3 Material properties of Water

Mass density	Bulk modulus
1000 kg/m^3	2.2 GPa

2.1.6 Beam orientation

Parts assigned with beam elements have to be assigned with orientations. Face sheets are assigned with default beam orientations for a 2D model. While assigning the beam orientation, direction of "a" dimension has to be the negative "z" direction which is the out of plane thickness of the model. Figure 2-2 below shows the orientation of face sheets. The arrows indicate axial direction of the beam.

Figure 2-2 Beam orientation

2.1.7 Analysis steps

Direct Steady State Analysis step

A steady state direct Step is created in order to perform a frequency response analysis for time-harmonic (sinusoidal) excitation. The frequency ranges studied for the modal analysis depends on the type of loadings applied on the model. For a loading type of Modified Ricker pulse, the range of frequency depends on the dominant frequency of the study. With an instantaneous loading type, frequency range is generally studied to be 1 Hz to 2000 Hz with 1500 points in between them on a linear scale. The scale and number of points considered are important in calculating accurate Sound Transmission Loss (STL) values.

The natural frequency extraction procedure based on solving an eigenvalue problem is conducted to find the natural frequencies and corresponding mode shapes of the structural model in vacuo (without fluid loading), and for the acoustic cavity with rigid walls This information helps to interpret the peaks and valleys exhibited in the STL frequency response curves. In the case of interactions with air, the coupling is weak and the resonant peaks in the frequency response due to excitation closely follow the natural frequencies of the vibrating structure in vacuo. Obtaining the natural frequencies from an eigenvalue extraction also helps bias the frequency response evaluation points towards

the natural frequencies. To simply the analysis, the Steady State Direct step with a linear scale as discussed earlier is performed.

For transient analysis, a Dynamic explicit step is created to conduct a time-dependent analysis procedure. The value of final time in a Dynamic explicit step is dependent on the type of excitation loading considered. The number of time increments within that time period for the analysis for accurate results is handled internally by ABAQUS based on the mesh size and material properties for wave speeds, which is the default automated time-stepping scheme.

2.1.8 Assembly

The assemblies of structural parts are coupled with the acoustic fluid domains using tie-constraints in ABAQUS. For a Fluid-Structure interaction, care must be taken to choose the Master and slave surfaces. The master surface will be assigned to structure with higher wave speeds and will have a relative coarser mesh. The slave surface has a lower wave speed and smaller characteristic wave lengths, which requires a finer mesh for accuracy. Hence face sheets are chosen to be the master surfaces, and the surface of fluid domain as slave.

2.1.9 Mesh

Face sheets are assigned with B22 beam elements based on Timoshenko beam theory in ABAQUS. Timoshenko beam theory captures the transverse shear deformations in the face sheets and applies to a length to height ratio greater than 8 times.

The fluid parts are assigned 2D acoustic mesh elements to capture the acoustic pressure values. AC2D3 elements, which is a 3-node 2D acoustic triangle type is used to mesh the fluid domain. Mesh size is biased to have more elements towards the Fluid-Structure boundary. This is done considering the need to calculate STL near the interface with a high accuracy.

2.1.10 Acoustic pressure load

For models with air on the incident side, the incident incoming acoustic plane-wave is applied as a time harmonic loading with uniform pressure amplitude applied on the lower face sheet as shown in the Figure 2-3. . When a uniform pressure amplitude load is specified in this way, the load amplitude is doubled to account for the rigid blocked pressure due to back-scattering which for an air-backed panel is equal to the amplitude of the incident wave pressure [1]. For the case when water is interacting on the incident side, the exterior acoustic region on the incident side of the structure is modeled with NRBC's similar to the transmitted side. The acoustic plane wave excitation is modeled in ABAQUS using a scattered field with wave loading with interactions on both the interacting acoustic surface and the structural surface. Wave interactions are also specified on the incident side rigid baffle surfaces. The direction of the plane-wave is specified by defining a source target reference point on the interacting surface.

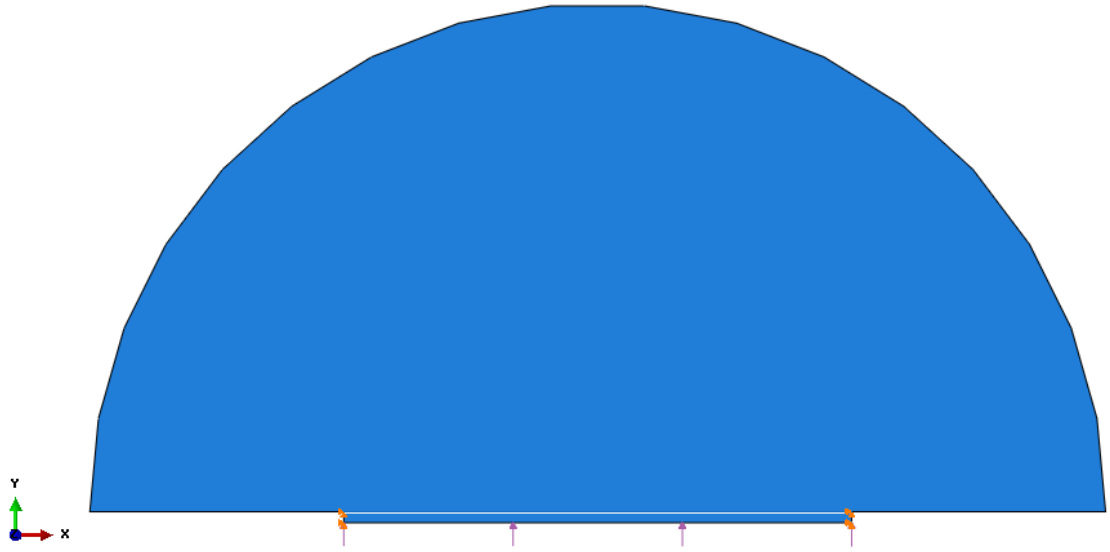

Figure 2-3 Load with a uniform pressure

For transient analysis of a time-dependent plane-wave pulse, a Modified Ricker Pulse with a dominant frequency [15] is applied for a time-dependent Dynamic Explicit analysis

$$v(t) = \begin{cases} \frac{(0.25u^2 - 0.5)e^{-0.25u^2} - 13e^{-13.5}}{0.5 + 13e^{-13.5}} & \text{when } 0 \le t \le \frac{6\sqrt{6}}{\omega} \\ 0 & \text{otherwise} \end{cases} \qquad (2.1)$$

Where $u = \omega_r t - 3\sqrt{6}$ is the dominant frequency of excitation

Figure 2-5 plots the Modified Ricker pulse and the amplitude of its Fourier transform in Figure 2-5. It can be observed that the Fourier transform has a single well defined central frequency ω_r and has non-zero values only over a narrow frequency range.

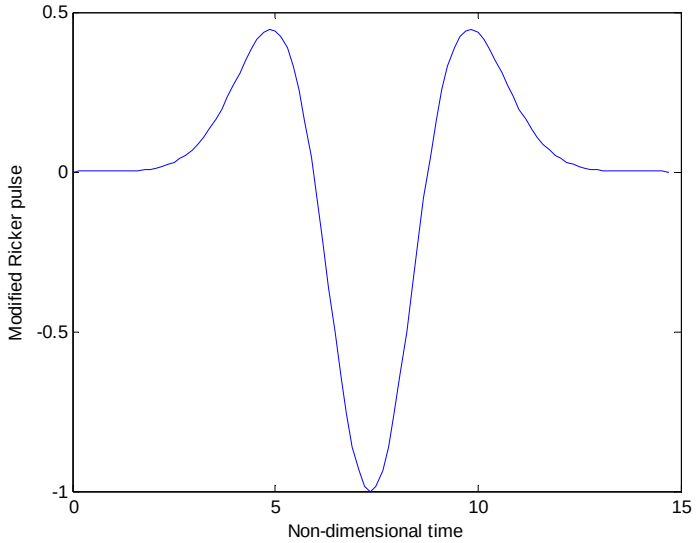

Figure 2-4 Modified Ricker Pulse vs normalized time **ω**rt

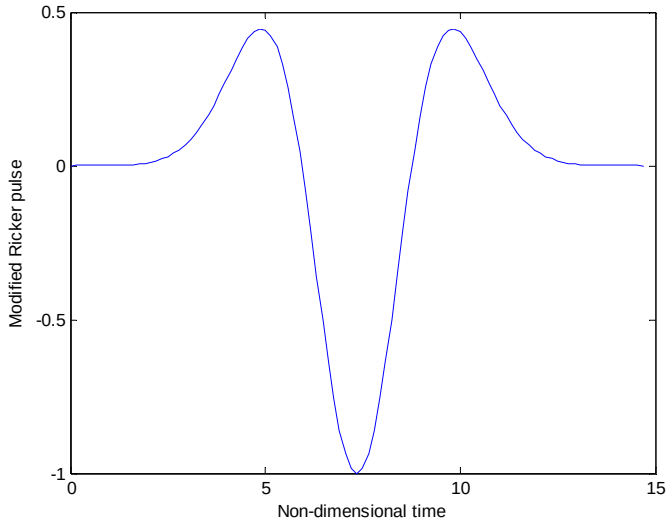

Figure 2-5 Fourier transform of Modified Ricker pulse. The amplitude spectrum vs frequency **ω**/**ω**r.

Another dynamic excitation considered is a periodic sinusoidal loading of frequency 100 Hz, is applied for a time-dependent transient analysis starting from zero. This introduces a transient solution which decays to a steady-state solution over time.

For direct steady-state frequency response analysis, a time-harmonic pressure excitation is specified over a range of frequencies from 1 to 2000 Hz, in enough frequency increments to resolve peak resonances in the response curves.

2.1.11 Boundary conditions

Figure 2-6 shows Face sheets have pinned boundary conditions; i.e. the ‘x’ and ‘y’ translations are zero. The rotational degree of freedom however, is free.

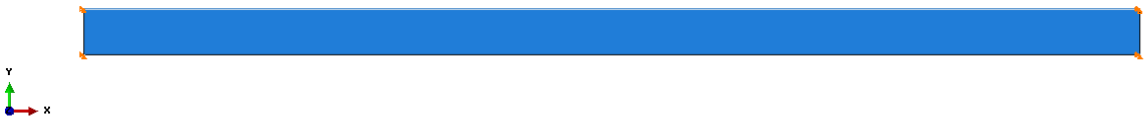

Figure 2-6 Boundary conditions

2.1.12 Sound Transmission Loss (STL) for structures interacting with air

An “.odb” file is created in ABAQUS containing the outputs of the analysis. The required output of interest is Acoustic pressure i.e. POR at the interface the transmitted side Face sheet and exterior Acoustic domain. A node set is created consisting of nodes at the interface. A history output request allows the user to request the POR values for all the frames for the specified node sets.

STL (dB) values are calculated using these POR values using

$$STL_{air} = 20\log_{10}\left(\frac{p_i}{p_t}\right) \tag{2.2}$$

where,

p_i is the Root Mean Square (RMS) value of pressure on the incident side (N/m^2)

p_t is the Root Mean Square (RMS) value of pressure on the transmitted side (N/m^2)

RMS values of p_i is calculated as shown below

$$p_i = \sqrt{\frac{p_1^2 + p_2^2 + ... + p_n^2}{n}} \tag{2.3}$$

Where $p_1, p_2, ..., p_n$ represents values of acoustic pressure of individual nodes on the incident side, and n is the number of nodes on the incident side.

Similarly the RMS values of P_t is calculated as shown below

$$p_t = \sqrt{\frac{p_1^2 + p_2^2 + ... + p_n^2}{n}} \tag{2.4}$$

Where $p_1, p_2, ..., p_n$, represent values of acoustic pressure of individual nodes on the transmitted side, and n is the number of nodes on the transmitted side.

2.1.13 STL of structures interacting with water and other fluid domains

The above method of finding the STL values using ratio of acoustic pressures in only valid if the structure is surrounded by Air on both sides. If one or both the Incident and

Transmitted sides are composed of different acoustic fluids, STL is more generally defined as the ratios of acoustic powers, with Incident power given by

$$P_i = \frac{1}{2}\frac{\tilde{p}_i^2}{\rho_i c_i} \tag{2.5}$$

where,

$\tilde{p}_i$ are the complex nodal values of the incident amplitude

ρ_i is the mass density of acoustic fluid in the Incident domain

c_i is the wave speed of sound in the acoustic fluid in the incident domain

The power on the transmitted surface of the acoustic domain is given by,

$$P_t = \frac{1}{2}\tilde{p}_t V_t' \tag{2.6}$$

where,

$\tilde{p}_t$ are the complex nodal values of the acoustic pressure on the transmitted side

V_t' is the conjugate of the complex values of the acoustic particle velocity on the transmitted surface.

Hence STL as ratio of powers is given by,

$$STL = 10 \log_{10} \left(\frac{P_i}{P_t} \right) \tag{2.7}$$

2.2 Acoustic response of a baffled plate to incident sound waves

The incident sound wave characteristic of the panel interacting with an acoustic fluid is of particular interest in the present study. To study the phenomenon of scattering of sound waves as a result of reflection from elastic panel surfaces of non-uniform specific acoustic impedance [1], the decomposition of the total pressure field into an elastic scattered and incident wave solution is needed. The impedance is the ratio of acoustic pressure to the normal velocity of the panel on the interacting surface. Analytical solutions write the elastic scattering solution as the sum of a rigid scattered solution and an elastic structural-borne sound radiation solution. This decomposition helps to understand the sound transmission characteristics, especially in modal analysis based analytical methods for acoustic response of flexible structures [1]. For analytical solution methods, the rigid scattering solution is imposed as an additional applied block pressure load in addition to the incident pressure applied to the elastic structural equations. The radiated pressure term adds a fluid impedance term to the elastic equations. For a flat elastic baffled panel, the added block pressure has the same amplitude as the incident pressure.

2.2.1 Effective scattering response to air incident field (Pressure load)

For a given panel interacting with air, the scattered pressure is small in comparison with the Incident sound pressure. However, as mentioned in the pressure load section, the

blocked pressure leads to a total force per unit length to be double that of an unobstructed incident sound pressure for Structures with Air in its incidence field [1]. This signifies that the effects of scattering wave phenomenon can be approximated without actually including an acoustic Air field on the incident side; hence reducing computational costs. Thus to approximate the STL characteristics we can include the scattering wave characteristics by either doubling the pressure load amplitude or halving the value of incident plane Sound wave in the STL calculations. Hence equation for STL becomes

$$STL_{air} = 20\log_{10}\left(\frac{p_{eff}}{p_t}\right) \tag{2.8}$$

$$\text{where } p_{eff} = \frac{p_i}{2} \tag{2.9}$$

Figure 2-7 compares STL values of a Double panel with scattering wave effects in incidence field and a Double panel with a surface pressure load. For the double panel with pressure load, effective scattering properties as discussed earlier is calculated using (2.8) and plotted. It can be noted that the dips or small peaks in resonances observed in Plane wave loading conditions is due to back scattering of reflected waves from both the panels and Air-cavity in between them. This comparison shows that the plane wave incident load can be approximated with good accuracy and less computational effort for air interaction on the incident side with a uniform pressure load with double the incident wave amplitude.

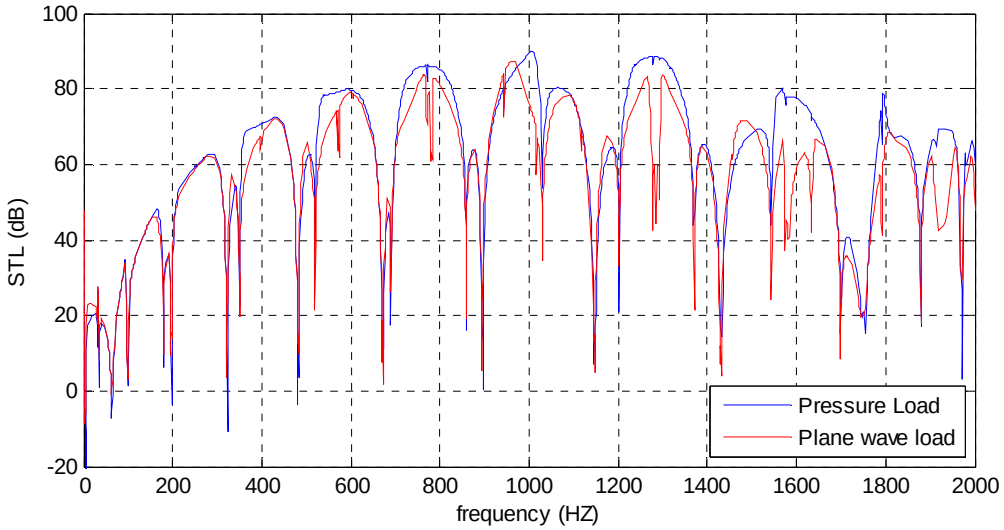

Figure 2-7 Comparison of STL values for a Double panel with pressure load (effective scattering) and Plane wave load

Figure 2-8 plots the STL values for a Regular Honeycomb sandwich panel (specific geometry to be discussed later) with a surface pressure loading and its effective scattering compared with a plane wave and its exact scattering effects. Again, comparison of solutions shows good agreement between the exact and approximate load condition.

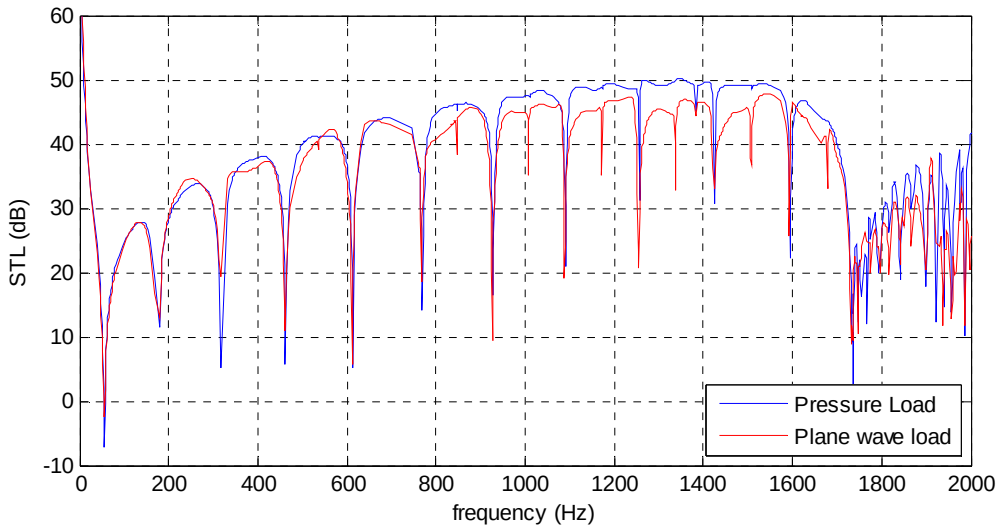

Figure 2-8 Comparison STL Honeycomb Sandwich Panel with pressure load (effective scattering) and Plane wave load

Figure 2-9 shows a plot for Regular Honeycomb sandwich panel for pressure loading with effective scattering due to blocked pressure compared to a plane wave loading type in vacuo. This comparison illustrates that when modeling the acoustic plane wave with a uniform load directly to the structure with no exterior acoustic interaction modeled, the STL is shifted higher, and the adjustment of double amplitude or use same amplitude but half effective incident in the STL ratio, must be made to account for acoustic block pressure due to back-scattering, to obtain the correct STL amplitude. So to consider effective properties of an Air domain in the incident field and its scattering effects due to blocked pressure, henceforth the values of Incident acoustic pressure is doubled or the STL effective incident pressure is halved.

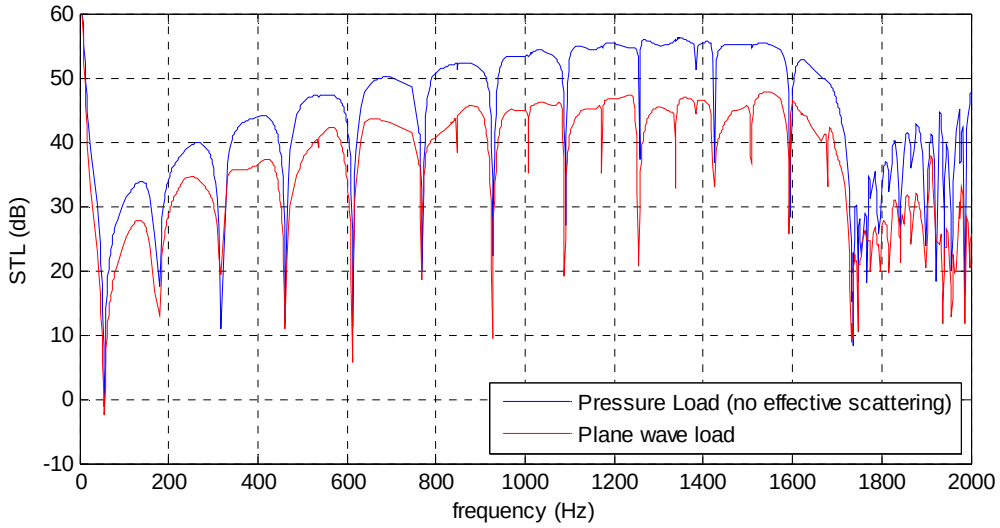

Figure 2-9 Comparison STL values improperly calculated (no effective scattering) Vs Plane wave load

CHAPTER 3: RESULTS AND DISCUSSION

3.1 Modes and natural frequencies

Figure 3-1 First mode of a simply supported beam at 4.63 Hz

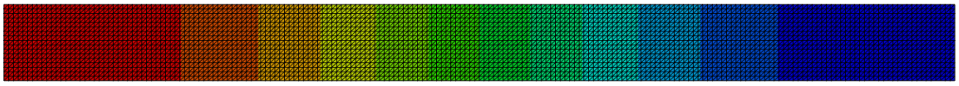

Figure 3-2 First mode at 85.15 Hz of a rectangular Air-cavity in between panels

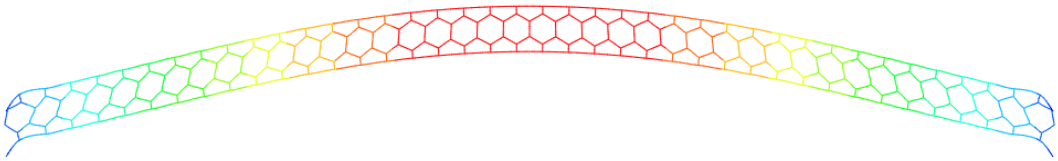

Figure 3-3 1st mode of a Honeycomb sandwich panel

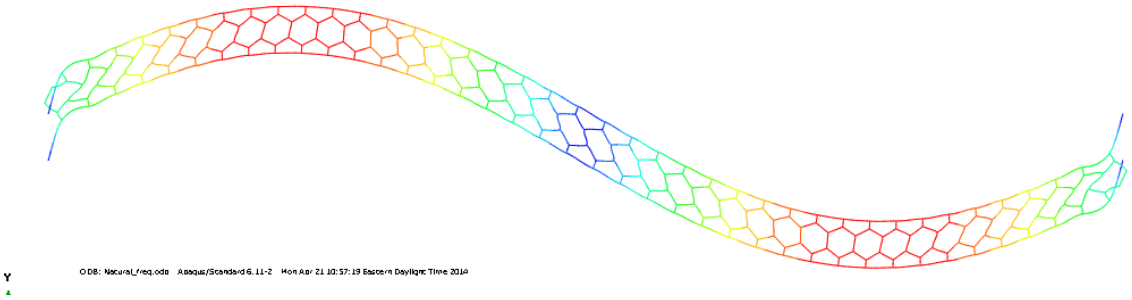

Figure 3-4 2nd mode of a Honeycomb sandwich panel

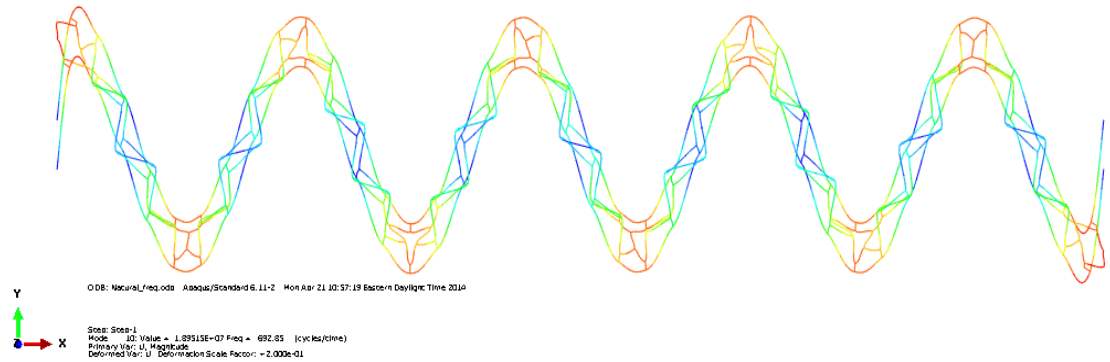

Figure 3-5 10th mode of a Honeycomb sandwich panel

3.1.1 Natural frequencies

The natural frequencies for Double panels with thicknesses of 0.006848 m and length 2 m and mass 73.96 kg with internal air cavity of depth 0.08667 m is given in (1.17) and (1.18). The tables contain natural frequencies found by ABAQUS and the natural frequencies calculated using analytical methods given in (3.1)

Table 4 Natural frequency convergence of Double panels in comparison with analytical solution

Mode number	Natural frequency (ABAQUS)	Natural frequency Analytical
1	4.00596	4.006043
2	16.0229	16.02417
3	36.048	36.05438
4	64.0766	64.09668
5	100.102	100.1511
6	144.116	144.2175
7	196.108	196.2961
8	256.067	256.3867
9	323.977	324.4895
10	399.825	400.6043

Table 5 Natural frequency convergence of Air-cavity of depth 0.08667 m in comparison with analytical solution

Mode number	Natural frequency (ABAQUS)	Natural frequency Analytical
1	85.7492	85.75006
2	171.493	171.5001
3	257.226	257.2502
4	342.944	343.0002
5	428.64	428.7503
6	514.31	514.5004
7	599.948	600.2504
8	685.549	686.0005
9	771.108	771.7505
10	856.619	857.5006

Table below is the natural frequencies of Regular and Auxetic Honeycomb model of length 2 m and height 0.08667 m with total mass of 73.96 kg.

Table 6 Natural frequencies of Regular and Auxetic honeycomb sandwich panel

mode number	Regular	Auxetic
1	63.1614	21.2633
2	130.506	42.6452
3	207.072	65.7934
4	284.611	89.6301
5	362.895	114.453
6	441.502	140.127
7	520.732	166.653
8	600.567	193.928
9	681.121	221.929
10	762.368	250.604

3.2 Single panel analysis

In order to better understand the interactions between fluid and structures in a finite baffle, it is important for us to understand a simple model setup in acoustic domain. A Single panel model of finite size of length 2m is simply supported surrounded by an acoustic domain on the transmitted side.

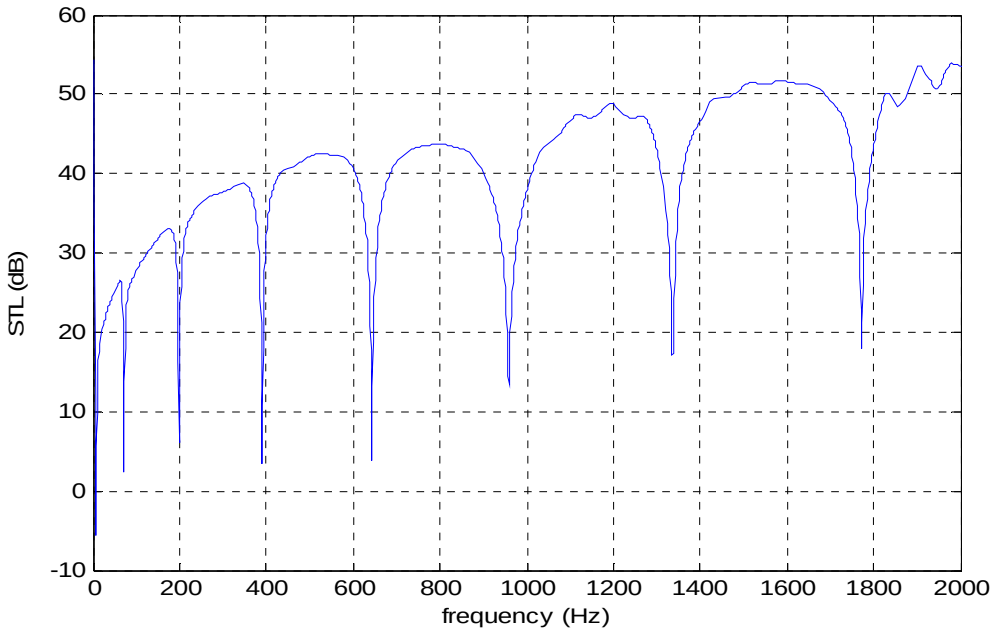

Figure 3-6 Single Panel with air on the transmitted side

3.3 Double panel analysis filled with air cavities

As mentioned earlier, the internal air-cavity resonances and its interactions with the incident and the transmitted panels play an important role in determining the STL characteristics. STL observed are dependent on the thickness, characteristic wavelength and bending wave speed of panels and on the depths of internal air-cavities in relationship with the acoustic spatial wavelength of sound in air.

Figure 3-7 plots the STL values in a double panel with an air cavity in between.

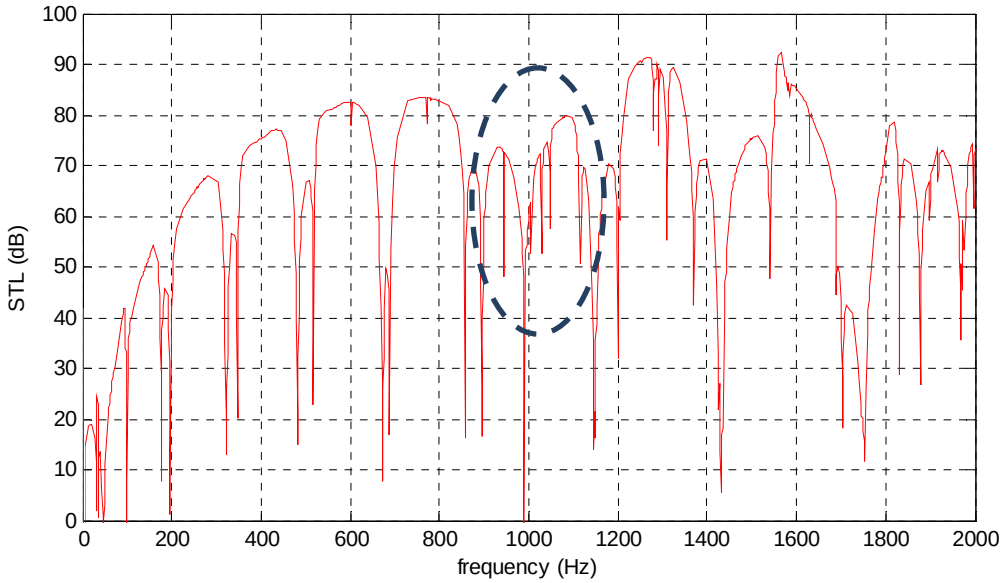

Figure 3-7 STL values of a Double Panel with Air Cavity depth to thickness ratio = 25.3125

The region up to the first depth resonant frequency is called as stiffness region. The first fundamental resonance is created by panels at 4.00596 Hz. The region where all the resonances for air-panel system are observed is called the resonance region. At a frequency of 85.15 Hz, the first natural frequency of internal air cavity is a dilatational resonance.

It is observed that since internal air-cavity is the only way the sound waves propagate from incident panel to the transmitted panel; acoustic resonances of air cavities are significant in the STL response of the panels. It can be noticed that, at frequency range 900 Hz – 1100 Hz, STL is reduced. This phenomenon can be directly correlated to the acoustic spatial wavelength of sound in air. If the wavelength of sound in air is twice the depth of air cavity‘d’, it is noticed that there is significant reduction in STL. In the above

model, it occurs at a frequency of 1000 Hz having a spatial wavelength of 0.3466 meters which is twice the depth of air-cavity. These wavelengths have zero vibration nodes in depth direction.

3.3.1 Effects of different depths to a constant thickness ratio on a uniform pressure load

The ratio of depths of acoustic air cavity to thickness of the beam is of considerable interest for maximizing STL for a particular range of frequencies. Figure below plots the STL values for different depths to thickness ratios. The thickness of the panels is a constant 0.006848m and depths of acoustic air cavity being 0.04334m, 0.08867m & 0.17334m.

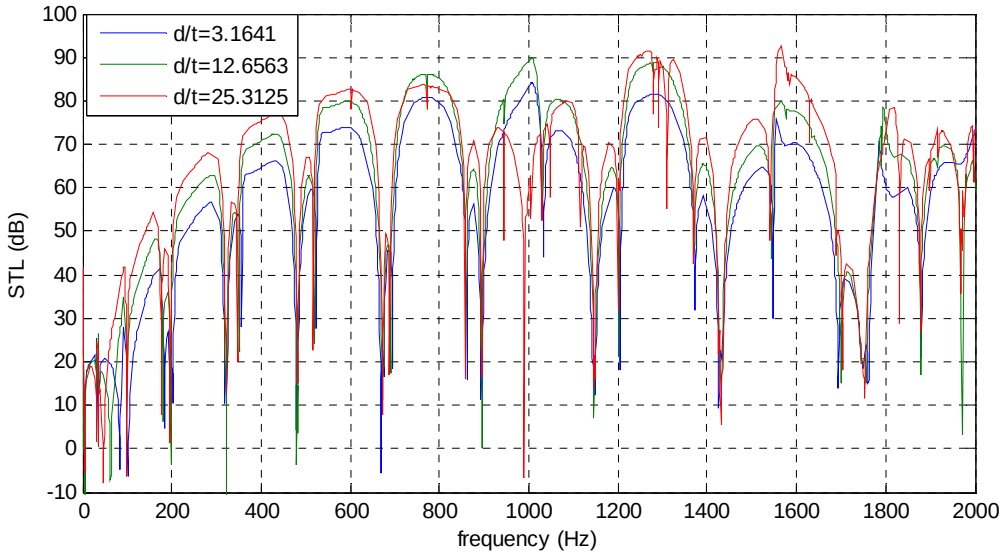

Figure 3-8 Sound transmission losses for a Double Panels with ratios of different acoustic Air Cavity depths to a constant Beam thickness

In the Figure 3-8, resonant and anti-resonant frequencies observed over the range up to 2000 Hz. The depth of acoustic air cavity plays an important role in determining the

effectiveness in blocking the sound for given particular frequency ranges. Larger the acoustic air cavity depth doesn't necessarily mean higher transmission losses. It can be observed that, within the stiffness region, maximum transmission losses are observed for panels with very small acoustic cavity depth. The STL values observed can be categorized for maximum losses by choosing ideal depth for acoustic air cavity based on targeted frequency ranges. In figure above, the highest d/t ratio of 25.3125 attains overall increased STL over the frequency range up to 2000Hz, except at frequency range from 895Hz to 1050Hz where it reduced. However, the other two models of d/t ratios 12.6563 & 3.1641 respectively show maximum transmission losses over that same range. This trend can be noticed for all the panels, with panel of d/t ratio 12.6563 showing least STL at 1960Hz and above.

Thus it is generalized that when the acoustic spatial wavelengths of particular frequencies of sound are twice the depth air-cavity thickness, given by $\lambda = 2d$, the STL values would reduce at those particular frequencies. These frequencies have zero vibration nodes in the depth direction of the air-cavities.

3.4 Triple panel analysis and comparison of STL with double and single panel

Structures with high stiffness and low mass have very good sound insulation properties over a large frequency band. Hence having multiple layers of thin panels in parallel with thin air gaps is effective instead of two or less panels with the same total mass. Figure 3-9 plots the triple panel model with thin air layers and Air on the transmitted side.

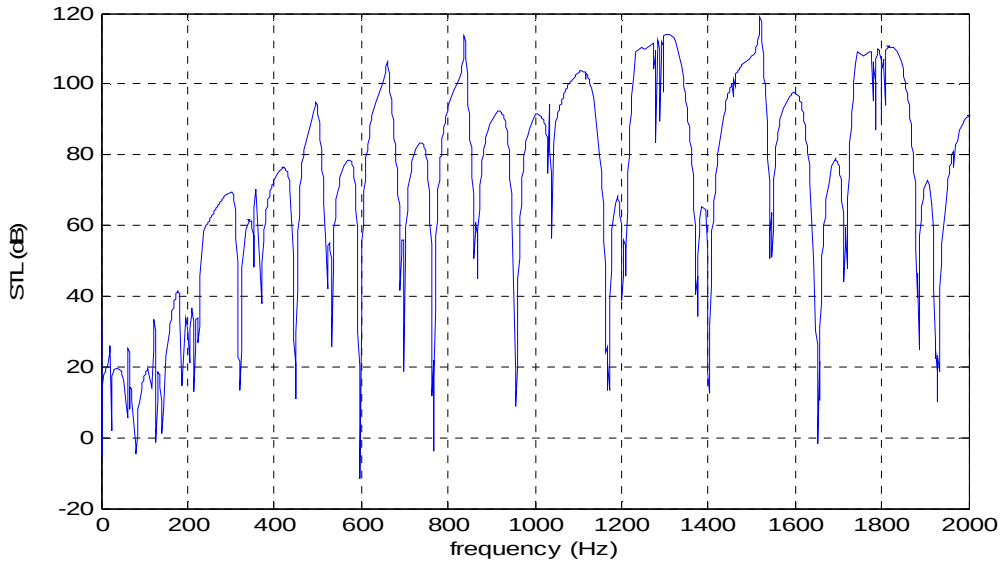

Figure 3-9 Triple panel with air layers in between and air on transmitted side

3.5 Air-cavity filled double and triple panels compared to single panel

Comparison between single panel, and air-filled double and triple panels are shown in Figure 3-10. It is noticed that, by introducing a column of air in between panels (double and triple), the overall STL is increased compared to single panel. The significance of air-cavity interaction with the structure and its sound insulation properties are of prime importance. More layers of thinner panels have stronger air-cavity interactions and hence introduce stronger air-borne resonances are noticed for triple panels. The increased overall STL in the triple panels can be attributed to increased effective stiffness.

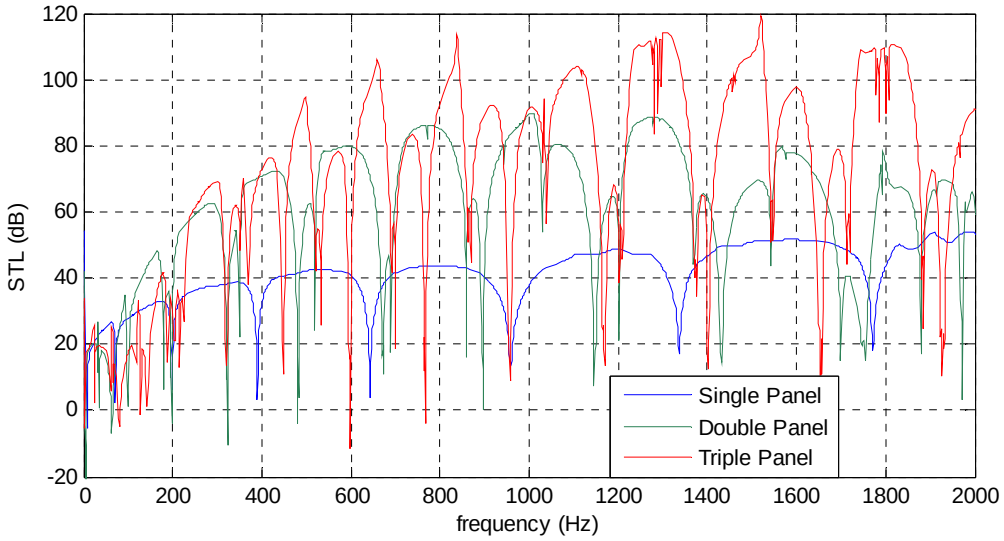

Figure 3-10 Comparison of Single, Double and Triple Panel models with air on the transmitted side

3.6 Effects of air-borne sound in panels with periodic connections

Air-borne sound in sandwich panels in general is neglected in analyzing transmission losses, assuming that Air with its low damping has negligible impact on sound transmission characteristics. Effects of including air-cavities in idealized “in vacuo” panels would significantly alter their vibro-acoustic behavior.

For a detailed understanding, we setup numerous models starting with finite double panels with rectangular cavity. Since there are no structural connections in between these panels, the coupling between the structure-air-borne sounds would be of prime significance. These double panels are then structurally connected by using studs, allowing a stronger interaction between panels along with air cavity coupling. Then cross-members are added to the sandwich panels adding more rigidity. All models are

designed for a constant mass. In all models, sound transmission characteristics are studied with and without having Air cavities in between for a clear understanding of air-structure coupling.

3.6.1 Double panel connected by multiple studs

A double panel connected by multiple studs as shown in Figure 3-11, is studied for its acoustic characteristics with and without Air-cavities in between them.

Figure 3-11 Double panels connected by studs

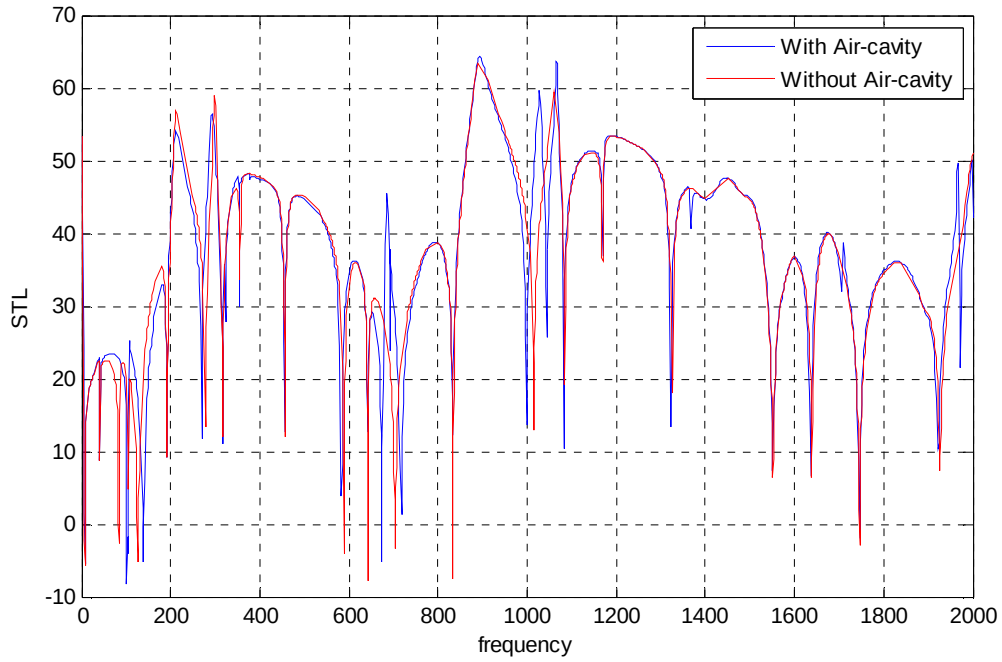

Figure 3-12 Comparison of STL values with and without Air-cavities in double panels connected by studs

The above figure compares STL values with Air-cavity and without Air-cavity in the double panels connected by studs. Data is obtained for natural frequencies of "in-vacuo" sandwich panel and air cavities respectively. The depth resonance occurring at 83.72 Hz is a sandwich panel resonance without Air-cavities in between, however it ceases to exist with having acoustic Air-cavities in between them as shown in the figure above. The latter mode is called a dilatational mode. The 2nd mode for at occurring at 685.5 Hz for air-cavities happens to be dilatational hence forming anti-resonance in the STL curve. These patterns are also noticed at higher frequencies. Such changes in the Vibro-acoustic behavior of the coupled Air-structure model make it compelling to further our

investigations. In order to make the coupling between the double panels stronger, we introduce cross-members in between those studs.

3.6.2 Double panels connected by studs and cross members

Figure below shows an abaqus model setup with cross-members added to the sandwich panel.

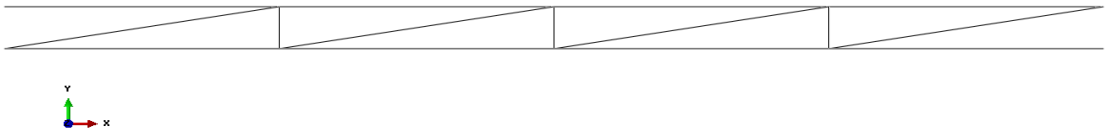

Figure 3-13 Double panels connected by studs and cross members

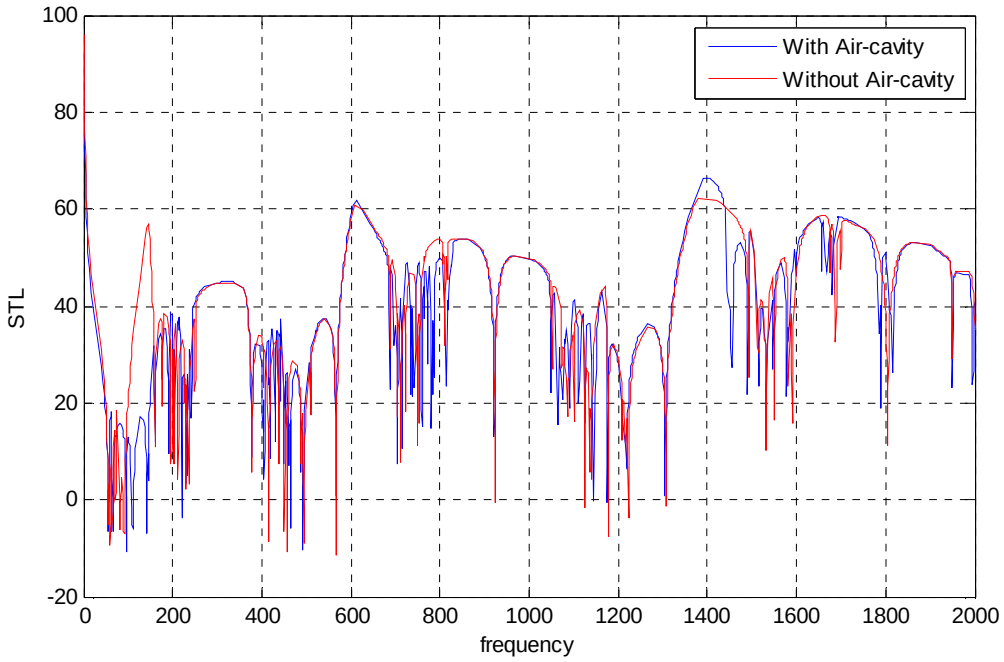

Figure 3-14 Comparison of STL values with and without Air-cavities in double panels connected by studs and cross members

For the sandwich panel shown in the above figure we expect the air-borne sound cause negligible variations in STL characteristics. However figure above shows it to be otherwise. We see that the difference with having Air-cavities and without air-cavities in the overall pattern of STL curve to be significant to say the least. To confirm with assurance the impact of not including acoustic air cavities we analyze the most widely used Honeycomb structures for their unique effective mechanical properties along with its sound transmission characteristics.

3.6.3 Honeycomb sandwich panel with air filled core cavities

Figure below shows the Abaqus model setup for a Honeycomb sandwich panel with cavities filled with air. This is a special case in which the boundary conditions are applied to the edges of honeycomb cores along with the face sheet panels.

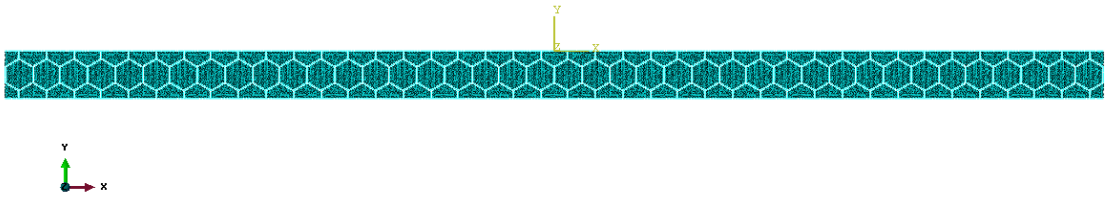

Figure 3-15 Regular Honeycomb sandwich panels with Air filled core cavities

We expect the STL to show minor differences with having air-cavities absorbing sound and interacting with adjacent structural surfaces. However, the sandwich panel with its low mass and high rigidity might play a pivotal role in absorbing the sound. Figure below plots the STL characteristics of two models one with Air-cavities and one without Air-cavities in between them.

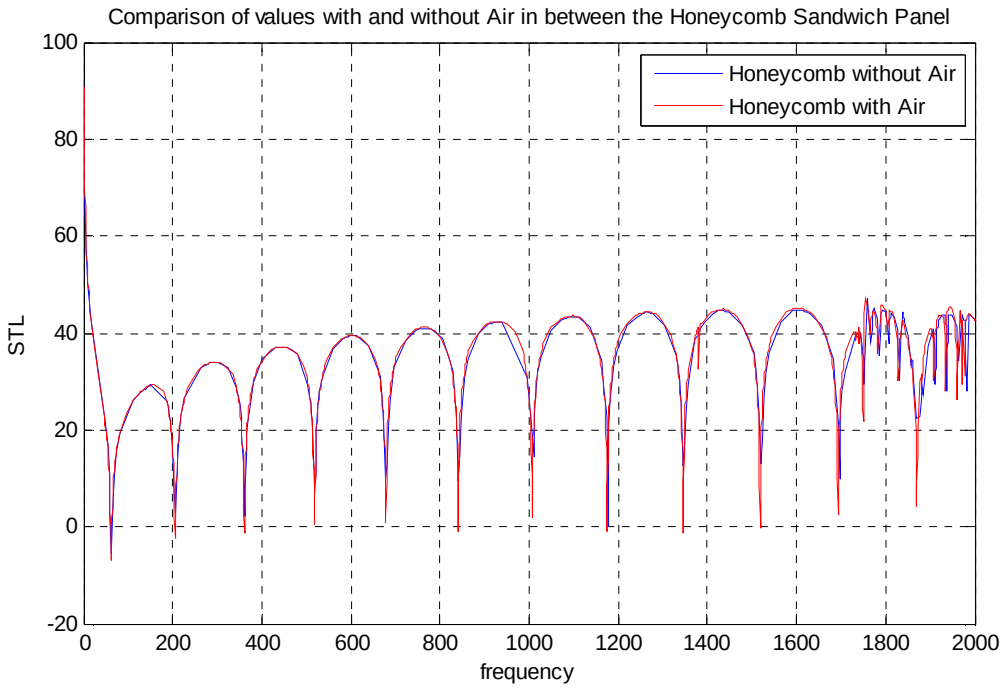

Figure 3-16 Comparison of STL values with and without Air filled core cavities of Honeycomb sandwich panels

In above figure, it can be noticed that because of a strong structural coupling introduced by cores in between the panels, most of the sound is absorbed by the sandwich panels. Inclusion of air-cavities in between these cores has negligible impact on the overall sound transmission characteristics. Air-cavity resonances occur at frequencies beyond our scope of interest. The 1st mode occurs at 3802 Hz and 2nd at 6233 Hz. Hence we expect any variations to occur at higher frequencies.

Introducing periodic connections in between the panels definitely improved the strength and stiffness in panels under other mechanical loads. But those structural connections in between the panels provide a structural path for sound to propagate strongly from

incident side panel to the transmitted side panel. Thus stronger structural coupling between panels allows easy propagation of sound from incident side acoustic domain to the transmitted side acoustic domain. This reduces the overall STL in panels. Such studies allows better understanding of the challenges involved in designing structures which are stronger under mechanical loads but also have good STL characteristics.

3.7 Auxetic honeycomb panels

3.7.1 Validation of STL values found using ratio of acoustic powers and acoustic pressures in an air field

According to theory, the STL is ratio of power given by (2.7) for any given incidence and transmitted acoustic domain. However, the STL of panels in Air field is simply the ratio of acoustic pressures given by (2.8) with effective properties of scattering incidence field of pressure load type and (2.2) for plane wave loaded scattering incidence field.

In order to validate our results found using ABAQUS, theoretically the STL values found by both the methods i.e. STL using ratio of acoustic pressures and STL using ratio of power surrounded by Air on both sides should match perfectly. Figure 3-17 and Figure 3-18 plots the STL curves for an Auxetic honeycomb sandwich panel with above conditions. As expected, the values of STL show an almost identical trend up to a frequency of 1350 Hz. Above 1350 Hz there are slight variations in the STL values for both methods which could be a computational inaccuracy. Hence the overall trends shown by both the methods prove the solutions to be accurate for the range of frequencies. This helps us to confidently explore the sound transmission characteristics of Sandwich panels in different acoustic fluids.

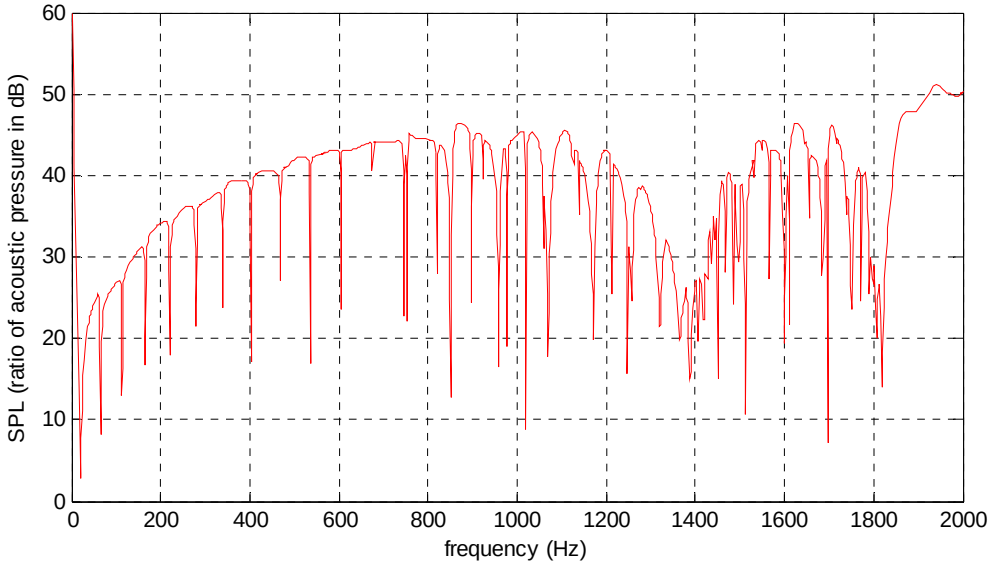

Figure 3-17 STL values calculated as ratio of acoustic pressures for Auxetic Honeycomb sandwich panel with Air on both sides

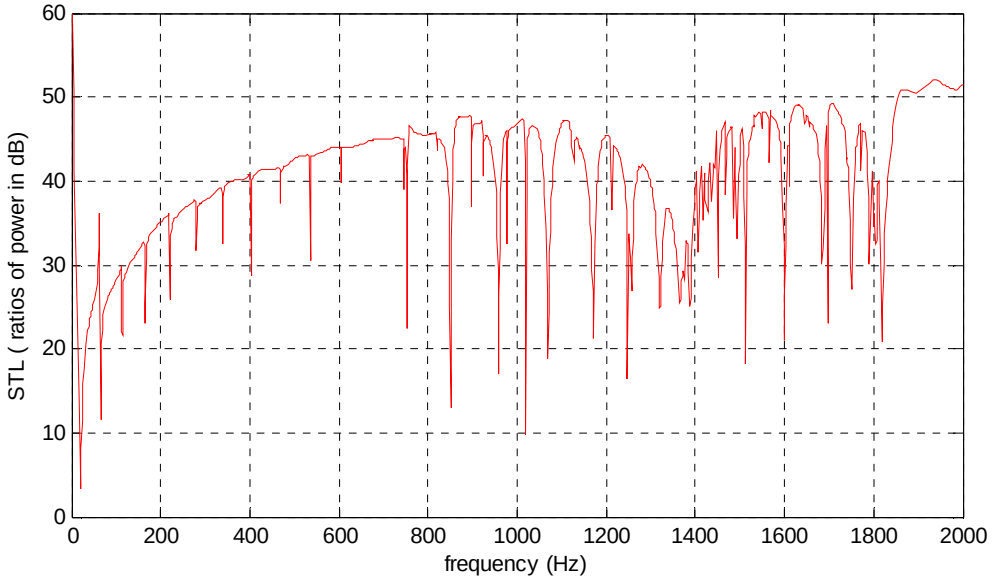

Figure 3-18 STL values as ratio of powers of Auxetic Honeycomb sandwich panel with Air on both sides

3.7.2 STL values with water on both incidence and transmitted field

Figure 3-19 plots the STL values for an Auxetic Honeycomb sandwich panel with water on both sides. Water has strong interactions with the surface of the sandwich panel. These interactions in turn will change the behavior of panels and significant damping is introduced. Hence there is a shift in natural frequencies of the panel. It can be noticed that the highest STL value observed is 17 dB while the overall STL values tend to remain below 9 dB for the range of frequencies. This means more sound got through the structure with water present on both sides of the acoustic domain. It can be noticed that at frequencies 750-800 Hz range there is significant loss relative to the overall trend.

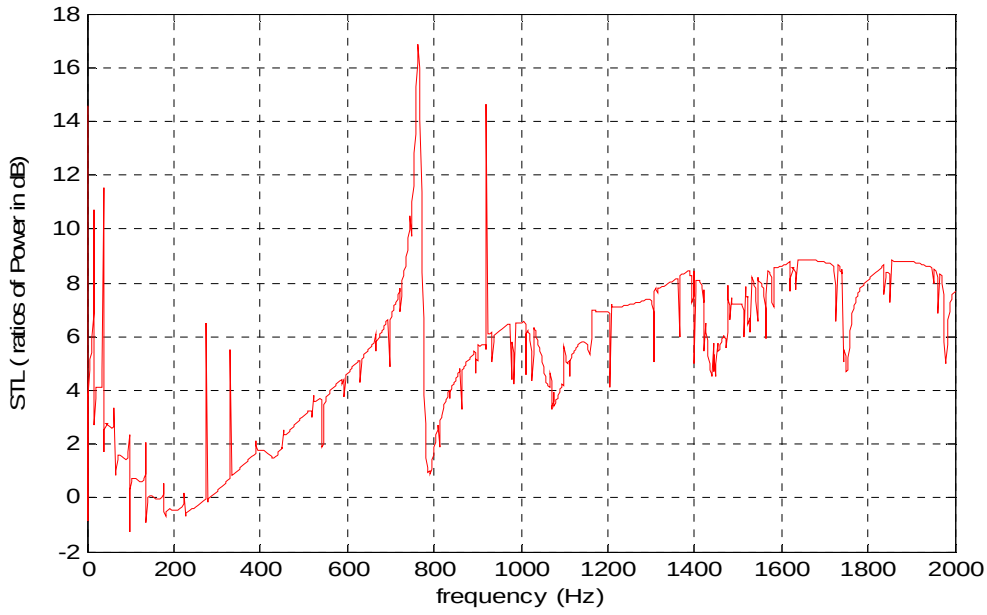

Figure 3-19 STL values of Auxetic Honeycomb sandwich panel with water on incident and transmitted field

3.7.3 Water on incident and air on transmitted side

Figure 3-20 plots the STL values for an Auxetic Honeycomb sandwich panel with water on the incident field and air on the transmitted field. The STL values are found to be in the range lesser than the Air-Air field case shown in Figure 3-18 and higher than the Water-Water field case shown in Figure 3-19. There is significant drop in the STL values for the range 800 Hz to 1100 Hz. Beyond 1100 Hz up to 2000 Hz there is a steady decrease in the STL values observed.

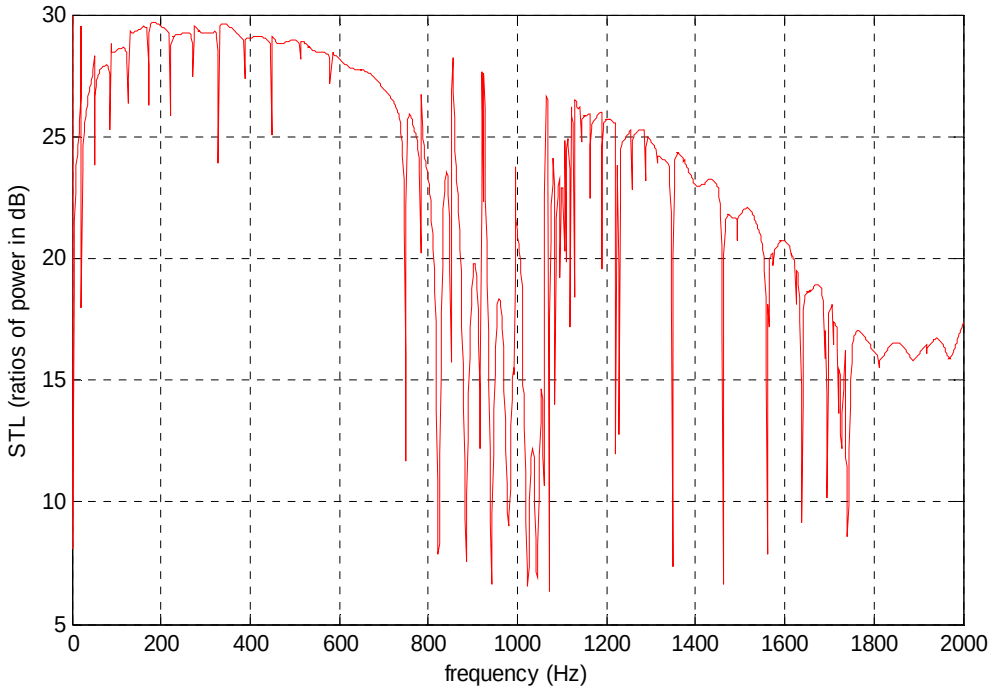

Figure 3-20 STL values of Auxetic Honeycomb sandwich panel with Water on Incident and Air on Transmitted field

3.7.4 Air on incident side and water on transmitted side

An Auxetic Honeycomb sandwich panel with air on the incident field and water on the transmitted field is studied for their sound transmission characteristics. Figure 3-21 plots the STL values over the range up to 2000 Hz. STL plot shows a similar behavior when compared to STL plot of water on the incident field and air on the transmitted field shown in Figure 3-20.

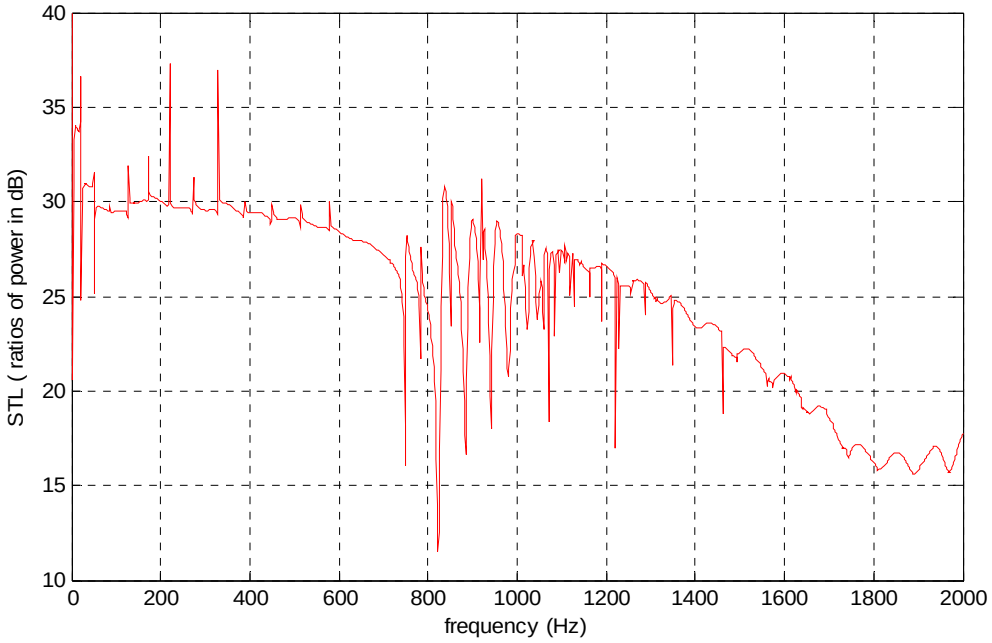

Figure 3-21 STL values of Auxetic Honeycomb sandwich panel with Air on Incident and Water on Transmitted field

3.8 Regular honeycomb sandwich panel

3.8.1 Air on both sides of acoustic domain

A Regular Honeycomb sandwich panel with air on both incident and transmitted fields is studied for its sound transmission characteristics. Figure 3-22, plots the STL values for range of frequencies up to 2000 Hz. First resonance occurs at 63.16 Hz which is also 1st mode of the sandwich panel. It follows that resonances at higher also are due to natural frequencies of the sandwich panel. These resonances are unaffected by the presence of air and its interactions with the sandwich panel.

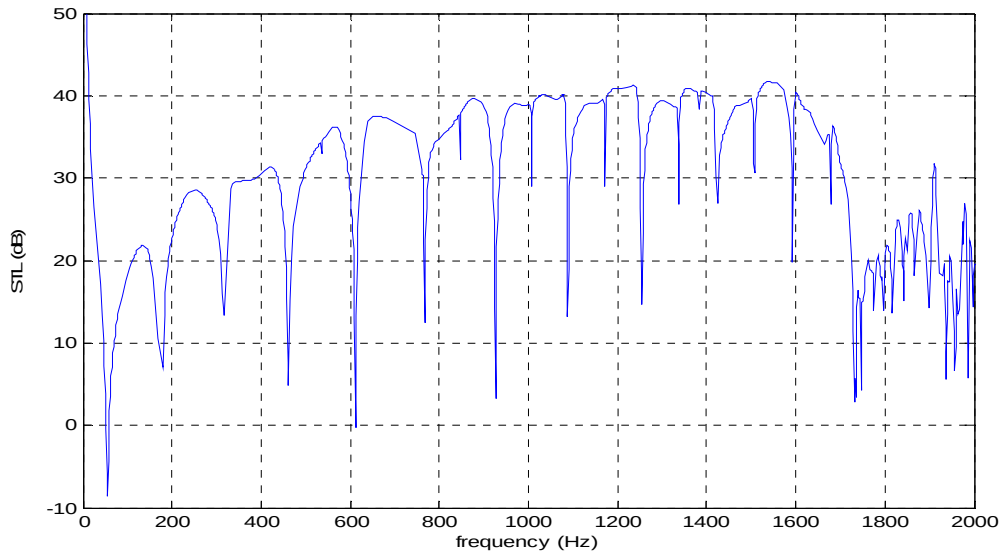

Figure 3-22 STL values for a Regular Honeycomb Sandwich panel with Air on both sides

3.8.2 Regular honeycomb sandwich panel with water on both sides of the acoustic domain

Figure 3-23 plots the STL values for a Regular honeycomb sandwich panel with water on both Incident and transmitted fields. It is observed that since water is of higher mass and has stronger interactions with the sandwich panel. This introduces significant amount of damping in the sound characteristics and the resonances observed are no longer driven by structural frequencies only. Resonances and anti-resonances are present over the range of frequencies.

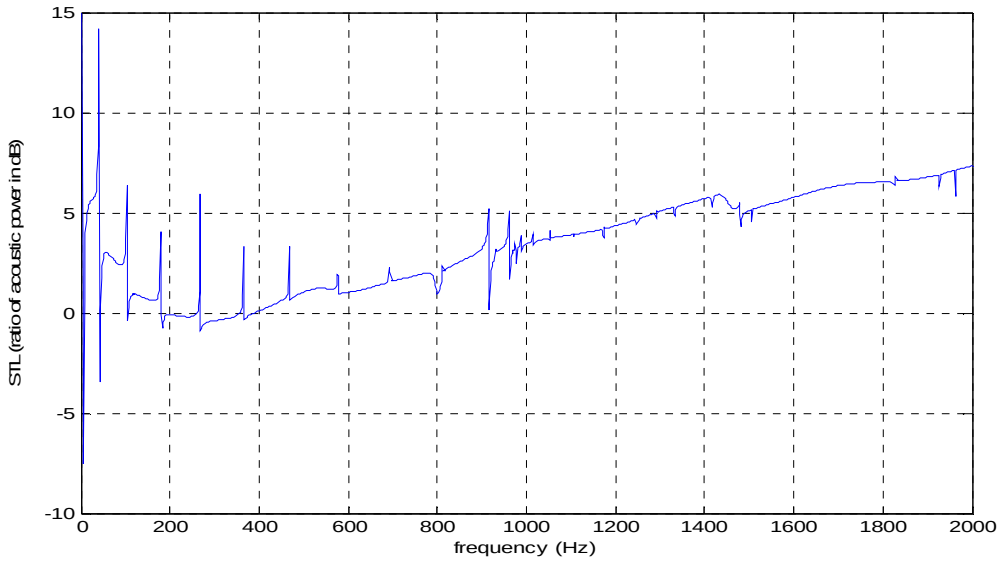

Figure 3-23 STL values of Regular Honeycomb sandwich panel with Water on both fields

3.8.3 Regular honeycomb sandwich panel with air on incident field and water on transmitted field

Figure 3-24 plots the STL values for a regular Honeycomb sandwich panel with air on the incident field and water on the transmitted field. Similar to Auxetic Honeycomb sandwich panels, the mix-match of acoustic fluids in case of Regular Honeycomb sandwich panels also show similar results. The Air-Water case has lower STL compared to Air-Air case Figure 3-22 and higher STL compared to Water-Water case Figure 3-23. In the lower range of frequencies anti-resonances are observed with normal resonances are more pronounced at higher resonances.

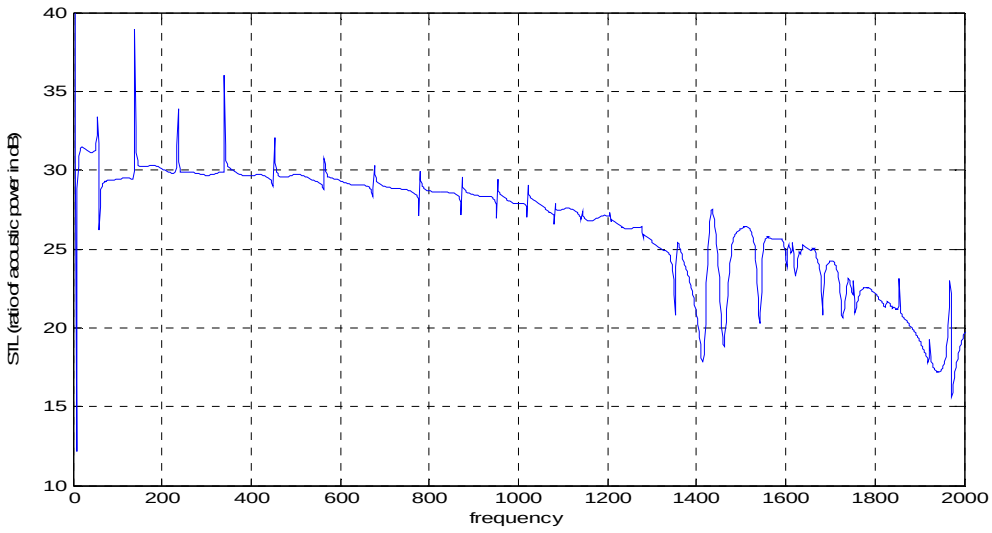

Figure 3-24 STL values for Regular Honeycomb sandwich panel with Air on Incident & Water on transmitted field

3.8.4 Regular honeycomb with water on incident and air on transmitted side

Figure 3-25 plots a Regular Honeycomb sandwich panel with water on the incident side and air on the transmitted side. Unlike the anti-resonances seen in the Air-Water field case shown by Figure 3-24, resonances are seen in the Water-Air case.

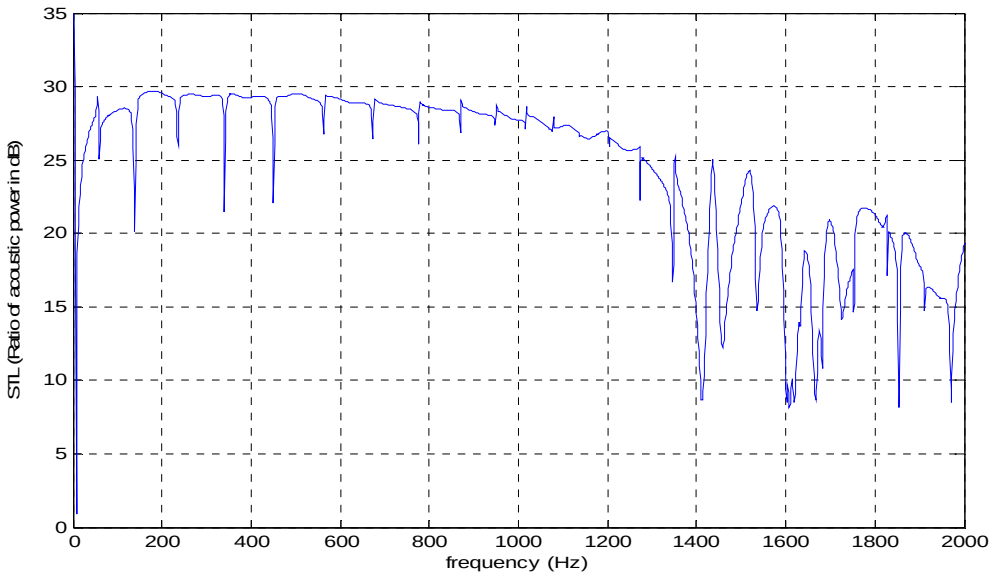

Figure 3-25 STL values for Regular Honeycomb sandwich panel with Water on Incident & Air on transmitted field

3.10 Comparison between auxetic and regular honeycomb sandwich panels

3.10.1 Comparison of regular and auxetic honeycomb sandwich panel with air on transmitted side and pressure loaded incidence

Figure 3-26 compares the STL plots of a pressure loaded Regular and Auxetic Honeycomb sandwich panels with Air on the transmitted side. For frequency range up to 800 Hz, the Auxetic model shows good sound insulation, however the higher frequency ranges up to 1600 Hz would be led by the Regular honeycomb model. Thus each both the models exhibit good insulation properties in a given frequency range.

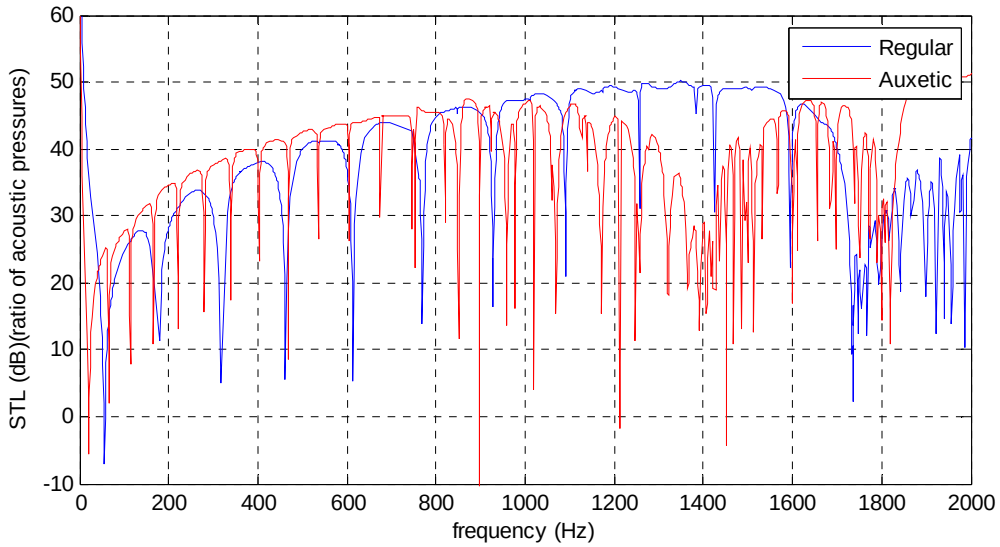

Figure 3-26 Comparison of STL plots of Pressure loaded Regular and Auxetic Honeycomb Sandwich Panel with Air on transmitted side

3.10.2 Comparison of regular and auxetic honeycomb sandwich panel with water on both incidence and transmitted fields

A Regular and Auxetic Honeycomb sandwich model with water on both scattering fields are compared for their sound insulation properties. Initially for a frequency range up to 200 Hz, Regular Honeycomb model shows good STL characteristics, but at higher frequencies the Auxetic Honeycomb model exhibits higher STL. Hence in case of Water-Water as Incidence/Transmitted fields, the Auxetic model exhibits higher STL over the range of frequencies studied.

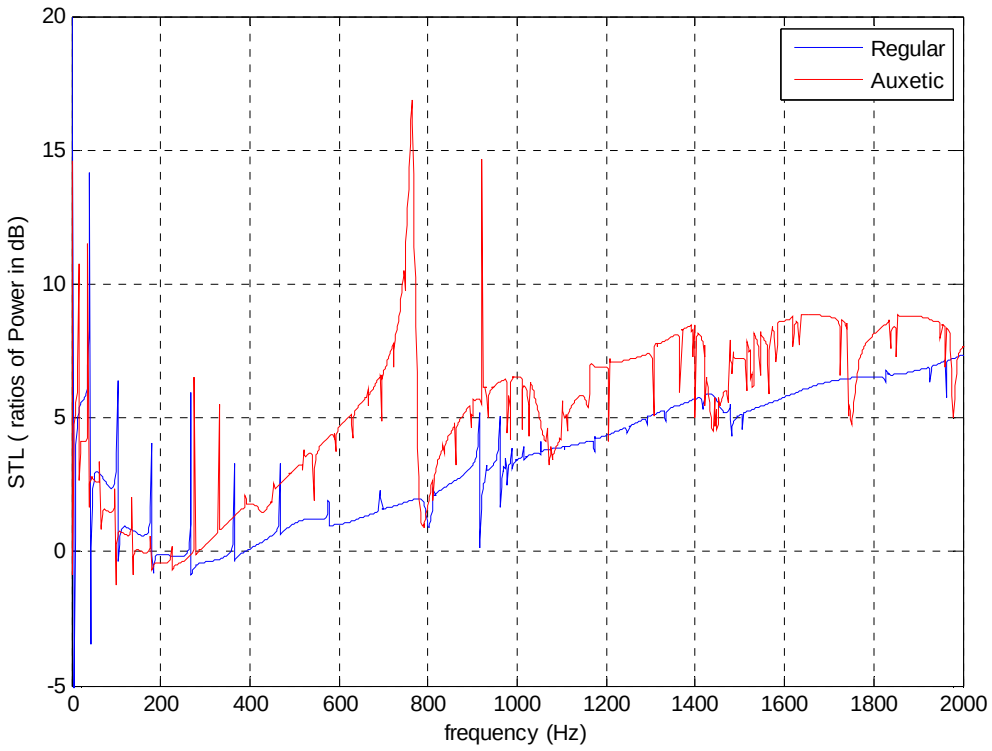

Figure 3-27 Comparison of STL plots of Regular and Auxetic Honeycomb Sandwich panel with water on both sides

3.10.3 Comparison of regular and auxetic honeycomb sandwich panel with water on incident field and air on transmitted field

Figure 3-28 plots the STL values of a Regular and Auxetic Honeycomb sandwich panel with water on the incidence field and air on the transmitted fields. While in all the earlier cases Auxetic model showed good sound insulation properties, however in this case STL is higher in Regular Honeycomb model.

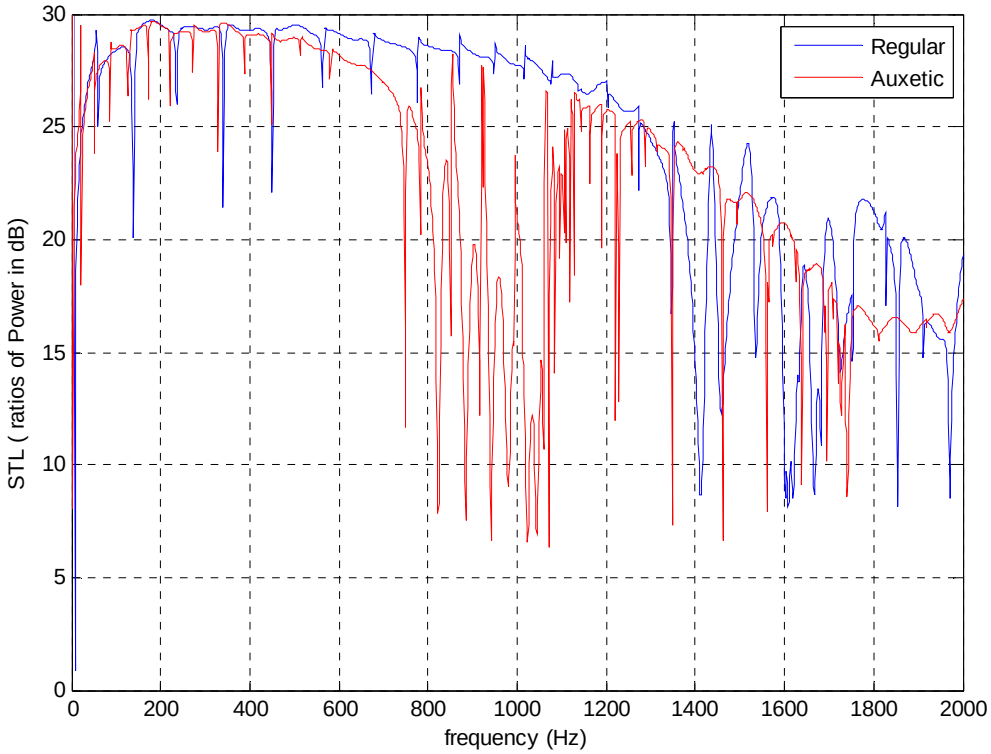

Figure 3-28 Comparison of STL plots of Regular and Auxetic Honeycomb Sandwich Panel with water on Incidence field and Air on Transmitted field

3.10.4 Comparison of regular and auxetic honeycomb sandwich panel with air on incident side and water on transmitted side.

In this section we compare the STL values of a Regular and Auxetic Honeycomb sandwich panel with air on the incident side and water on the transmitted side given by Figure 3-29. Unlike for Air-Water fields where Regular Honeycomb panel clearly showed higher STL, in case of Water-Air fields there are frequency ranges where each of the models exhibit higher STL.

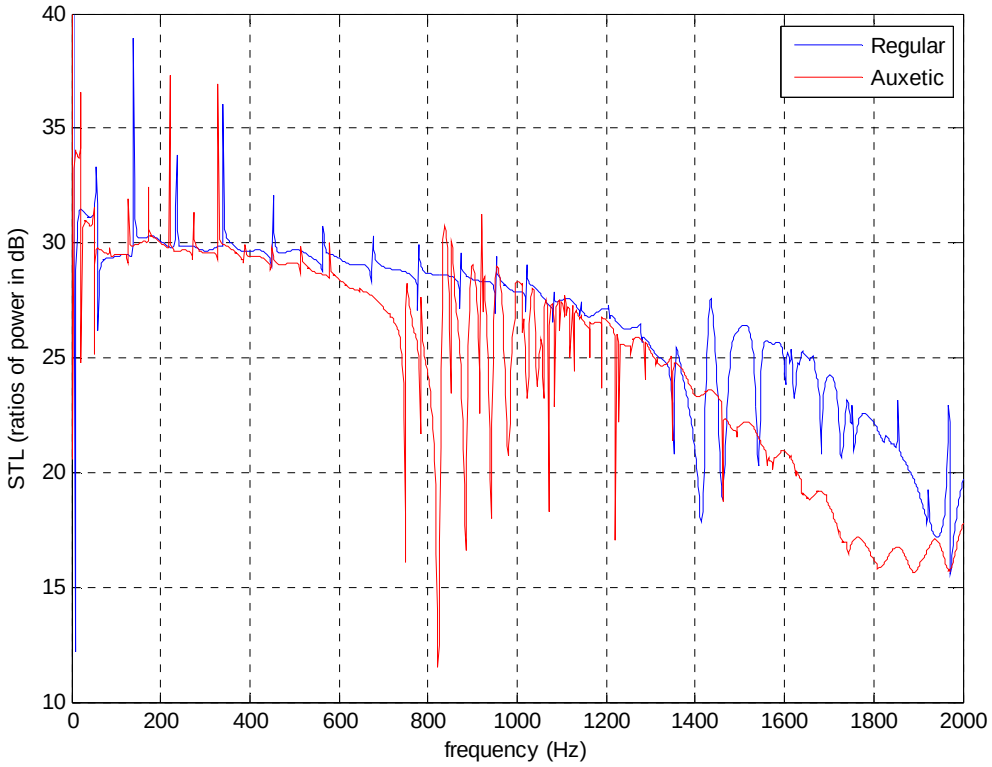

Figure 3-29 Comparison of STL plots of Regular and Auxetic Honeycomb Sandwich Panel with Air on Incidence field and Water on Transmitted field

3.11 Comparison of acoustic pressures on honeycomb sandwich panels loaded with a plane wave interaction of Modified Ricker pulse (Transient analysis)

In this section, a time-dependent dynamic explicit analysis is conducted on Honeycomb sandwich panels loaded with a modified Ricker pulse interaction wave(2.1). The dominant frequency of excitation is 100 Hz. The acoustic regions on the incident and transmitted side studied are Air-Air Figure 3-30 and Water-Water Figure 3-31 combinations. Comparisons are made between acoustic pressure values on the transmitted side for Auxetic and Regular Honeycomb sandwich panels.

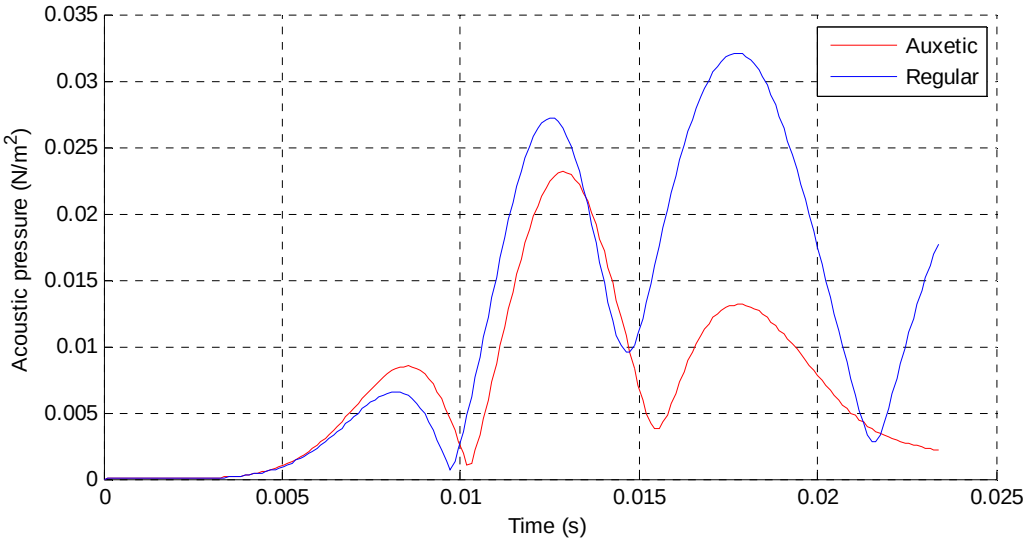

Figure 3-30 Comparison of Acoustic pressure on the transmitted side of Regular and Auxetic Honeycomb sandwich panel with Air on both sides

Figure 3-30 plots the acoustic pressures for honeycomb panels with air on incident and transmitted field. It can be noticed that the overall acoustic pressure is higher in Regular model which can be directly correlated to the time-harmonic steady state frequency

analysis studied in the earlier section Figure 3-26. It was found; the STL values are higher for Auxetic model at the dominant frequency of 100Hz and frequencies up to 400 Hz.

Figure 3-31 plots the acoustic pressures on the transmitted side for Regular and Auxetic Honeycomb sandwich panel with water on both sides of acoustic domain. In this case however, the acoustic pressures for Auxetic Honeycomb panel are higher, meaning lower STL values shown in Figure 3-27, consistent with the steady state frequency analysis. It is also observed that the transmitted pressure for the water interaction is of the order 10 times higher than the interaction with air. This result is also consistent with the much lower STL found for water compared to air in the steady-state response.

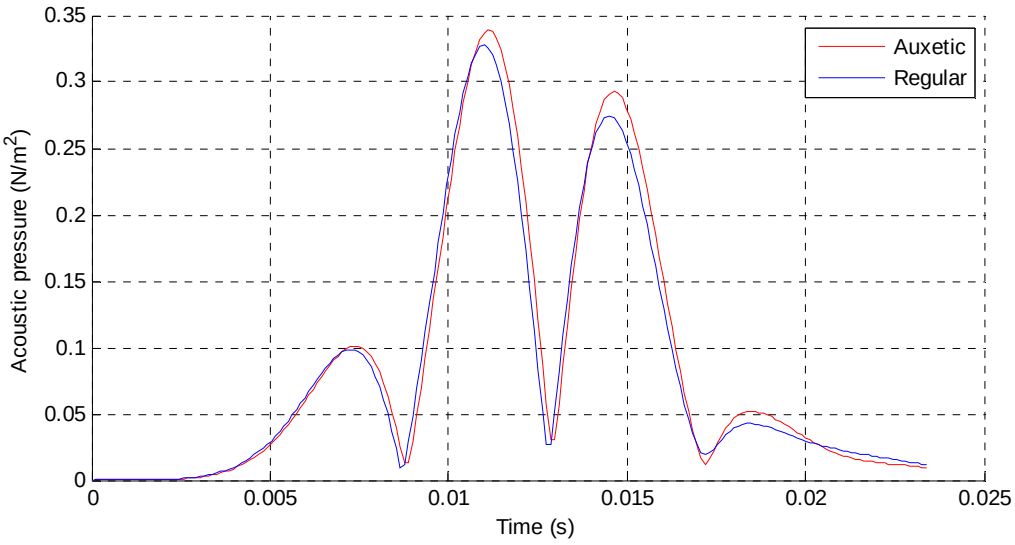

Figure 3-31 Comparison of acoustic pressure on the transmitted side of Regular and Auxetic Honeycomb sandwich panel with water on both sides

3.12 Comparison of acoustic pressures vs. time for a periodic sinusoidal load of 100 Hz

A periodic sinusoidal load of 100 Hz is applied as an interaction wave on the Regular and Auxetic Honeycomb sandwich panel. The acoustic regions on the incident and transmitted side studied are Air-Air Figure 3-32 and Water-Water combinations Figure 3-33. Acoustic pressure values on the transmitted side are compared in each of these cases.

Acoustic pressures in Figure 3-32 are plotted for an Air-Air case. The acoustic pressures for Auxetic Honeycomb model is lower than the Regular model which shows as a higher STL in Auxetic model in the steady state frequency response shown in Figure 3-26. While in Water-Water case, acoustic pressures are almost similar for Auxetic model compared to Regular model, leading to similar STL in Regular and Auxetic model shown in Figure 3-27. It is also noted that for water interaction with higher speed of sound, acoustic energy is radiated to the far-field through the NRBC faster than air, and thus the transient part of the sinusoidal pressure load starting from zero rapidly decays leaving the steady solution at the steady 100 Hz frequency. In the case of air, the transient part of the solution has not decayed significantly in the time interval studied up to 0.06 seconds, and appears that significantly more time would be needed for the transmitted solution to decay to a steady-state value.

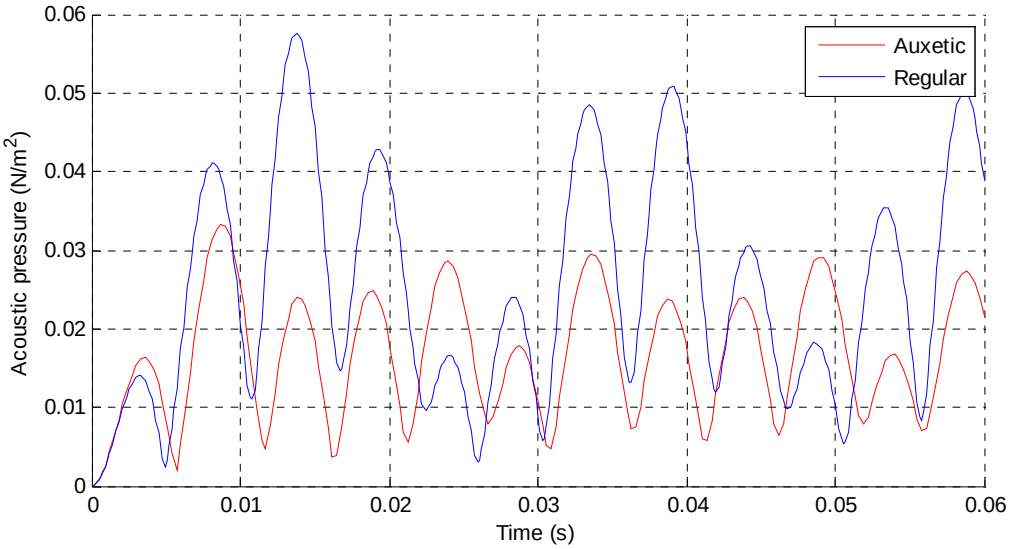

Figure 3-32 Acoustic pressure on transmitted side vs. time for Honeycomb panels with Air on both sides and periodic Sinusoidal load of 100 Hz

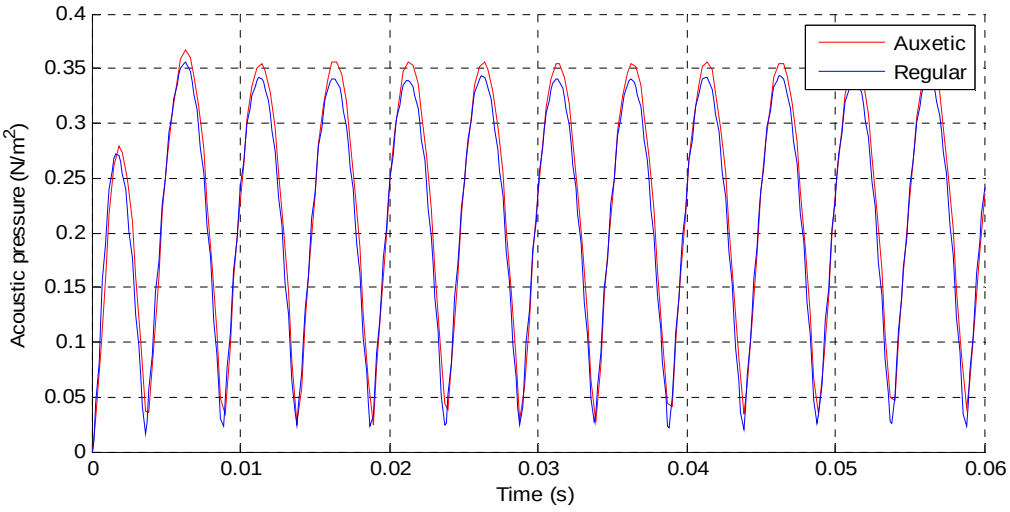

Figure 3-33 Acoustic pressure on transmitted side vs. time for Honeycomb panels with Water on both sides and periodic Sinusoidal load of 100 Hz

CHAPTER 4: CONCLUSIONS

4.1 Effects of air-cavity depths on STL in relationship with acoustic wavelength

Internal Air-cavity vibrations have significant impact on the STL characteristics of double panels. Air cavity resonances occurring at their natural frequencies are dependent on the geometric dimensions and material properties of Air. STL responses for different depths of air cavities in relationship to acoustic wavelengths are studied. Results showed that when the wavelength is twice the depth of the Air-cavity, the STL is reduced implying that an increase in sound transmission associated with the fundamental resonance cavity frequency with zero vibration nodes in depth direction. This effect can be noticed for the Air-cavity depths of 0.08667 m and 0.17334 m at frequencies 2000 Hz, 1000Hz respectively. The Air-cavity depth of 0.04334 m shows similar STL results beyond frequency range of interest. It can be generalized that for any particular frequency of sound, with its wavelength twice the depth of the acoustic air cavity, the STL values reduce significantly.

4.2 Sound transmission in single, double and triple Panels

STL analysis of Single panel, and Air-filled Double and Triple Panels with same total mass and Air on the transmitted side are studied. Single panel showed lower STL compared to double and triple panels, implying that Air-cavities in Double and Triple panels exhibited significant sound absorption characteristics. Air-cavity interactions in layered panels play an important role in sound transmission. Results showed that more

layers of thinner panels exhibited stronger Air-cavity interactions showing stronger Air-cavity resonances in the frequency response for STL. Triple panels with thin layers of Air-cavities have higher effective stiffness and hence show higher STL for the range of frequencies discussed.

4.3 Effects of connecting the panels with periodic lattice structures

In earlier sections we discussed the sound transmission effects of panels connected by acoustic Air-cavities. By connecting panels with periodic lattice structures, increases the stiffness and strength of the panels necessary for other mechanical loads. However, overall STL is reduced since such connections provide a strong acoustical path for sound waves to propagate from panel on incident side to panel on the transmitted side. Results showed for frequencies up to 2000 Hz, STL values for double panel were varied from 70 to 80 dB and for Triple Panels STL values varied from 80 to 110 dB, while STL values for Regular and Auxetic Honeycomb were significantly reduced to 40-50 dB ranges.

The effects of Air-cavities with periodic connections between the panels introduce cavity resonances in the structure frequency response. However, cavity resonances do not significantly alter structure-borne sound radiation and overall STL characteristics. These studies help us understand the challenges in designing structures needed to exhibit good strength and rigidity along with higher sound insulation properties.

4.4 STL in honeycomb panels with air and water as the acoustic fluid domains

Honeycomb sandwich panels with Air on the incident and transmitted side is studied for a range up to 2000 Hz. For frequencies up to 1000 Hz, the Auxetic honeycomb panel exhibits higher STL than Regular Honeycomb. However, from 1000 Hz to 1600 Hz, Regular model showed higher STL than Auxetic model and above 1600 Hz, Regular had reduced STL.

We also investigated the interaction of water with honeycomb panels for which STL is ratios of acoustic powers. To accurately calculate and validate the measure of STL as a ratio of power, we validated the results for an Air case. Theoretically, finding STL as a ratio of power should exactly match STL as a ratio of acoustic pressures. Such a validation approved the accuracy of the Finite Element model analyzed using ABAQUS.

For the cases of Water on both sides of the Regular and Auxetic honeycomb panels, most sound transmission is observed, meaning reduced STL, while mix match cases of Air on the incident side, water on the transmitted side and water on the incident side, Air on the transmitted side had slightly lower STL than Air-Air cases. Comparisons are made between Auxetic and Regular Honeycomb panels with each of these cases. Comparisons showed that, in Water-Water case, Auxetic model showed higher STL than Regular and in mix-match cases of Air-Water and Water-Air, higher STL is observed in Regular over Auxetic.

4.5 Transient analysis of honeycomb panels

A transient analysis with a modified Ricker pulse loading and a Sinusoidal load on Regular and Auxetic Honeycomb panels is studied. Results showed that in case of modified Ricker pulse loading, for Air-Air case acoustic pressure for Auxetic is lower than Regular model correlating with higher STL in the steady state frequency response for Auxetic model. However, in Water-Water case that effect reversed with higher acoustic pressures in Auxetic over Regular model which showed as lower STL in Auxetic model.

For sinusoidal load driven at a frequency of 100 Hz, the Air-Air case, Auxetic model has higher acoustic pressure and the transient part of the solution does not decay significantly to a steady state solution in the interval studied. However, for Water-Water case the transient solution decays rapidly starting from zero leaving the steady state solution at a steady frequency of 100 Hz.

4.6 Future work

1. In this study reference cases of honeycomb core angles of ‘+30’ and ‘-30’ are studied. In order to maximize the STL characteristics of honeycomb panels with different fluid domains, a multi-objective design study with honeycomb core parameters as design variables can be investigated.
2. The natural frequencies of internal air cavities in between honeycomb cores in sandwich panels were observed at high frequencies above 3800 Hz. These natural frequencies can be seen as resonances and their significance in STL can be investigated.
3. In this study, the 2D model studied has in-plane honeycomb cores in between double panels. As an extension, out of plane honeycomb cores in between double panels can also be studied, requiring a 3D model for the analysis.
4. In this study, effects of air and water are studied as the external acoustic fluid domain in honeycomb panels. It would be interesting to study STL effects of panels for other fluid domains.
5. It was observed that connecting layered panels with periodic lattice connections reduced the STL characteristics; it would be interesting to study the sound transmission effects of composite panels with foam as internal cores which have good sound absorption and insulation properties while retaining strength and stiffness under other mechanical loads.

APPENDICES

Results of SPL plots of auxetic and regular honeycomb sandwich panel

4.6.1 Regular honeycomb sandwich panel with water on both sides of the acoustic domain

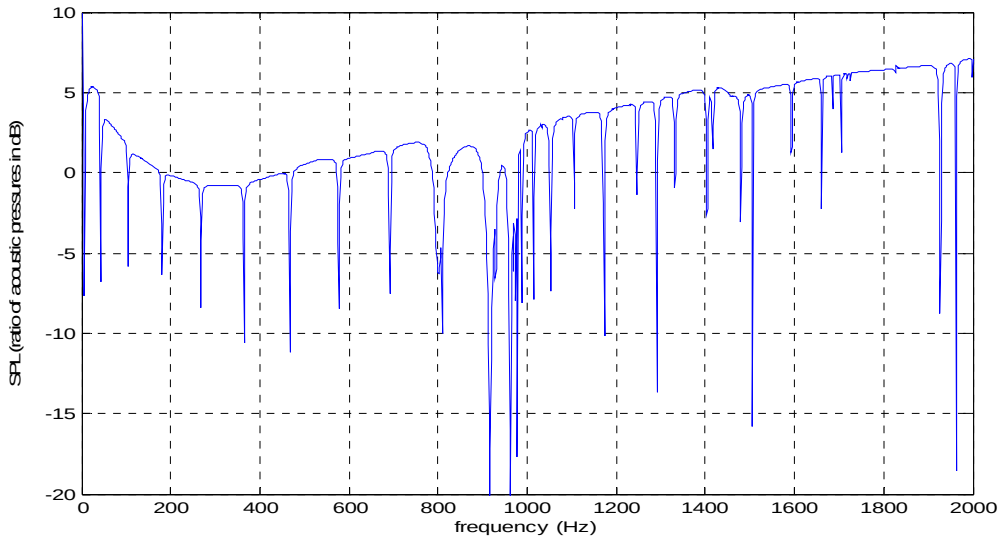

Figure 0-1 SPL values of Regular Honeycomb sandwich panel with water on both sides

4.6.2 Regular honeycomb sandwich panel with air on incident field and water on transmitted field

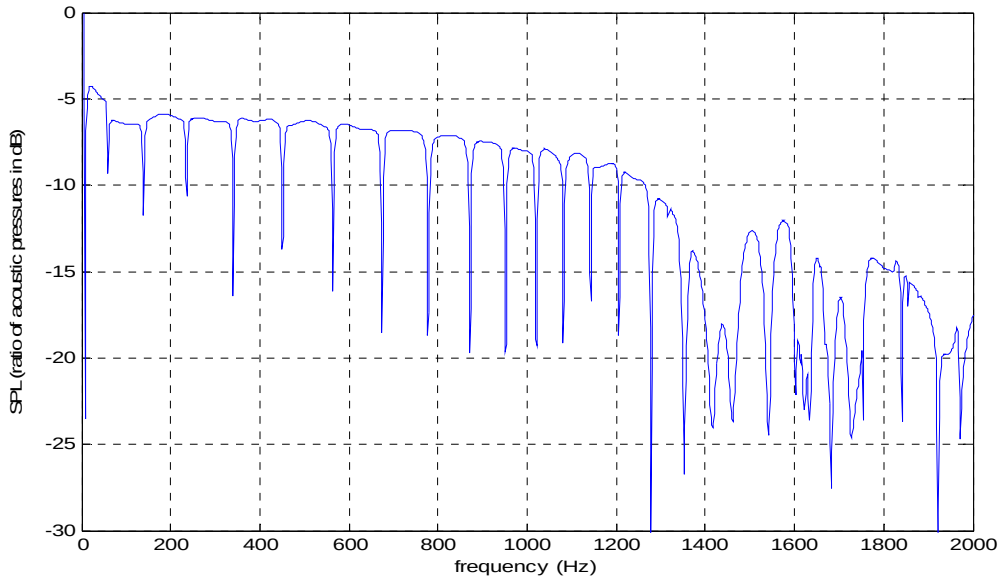

Figure 0-2 SPL values for Regular Honeycomb sandwich panel with Air on Incident & Water on transmitted

4.6.3 Regular honeycomb sandwich panel with air on incident field and water on transmitted field

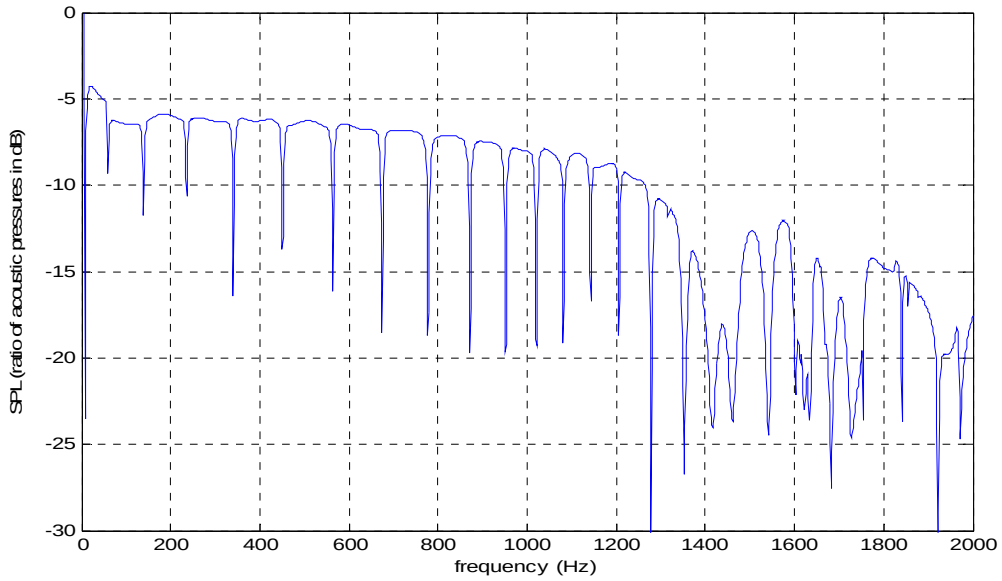

Figure 0-3 SPL values for Regular Honeycomb sandwich panel with Air on Incident & Water on transmitted field

4.6.4 Regular honeycomb with water on incident and air on transmitted side

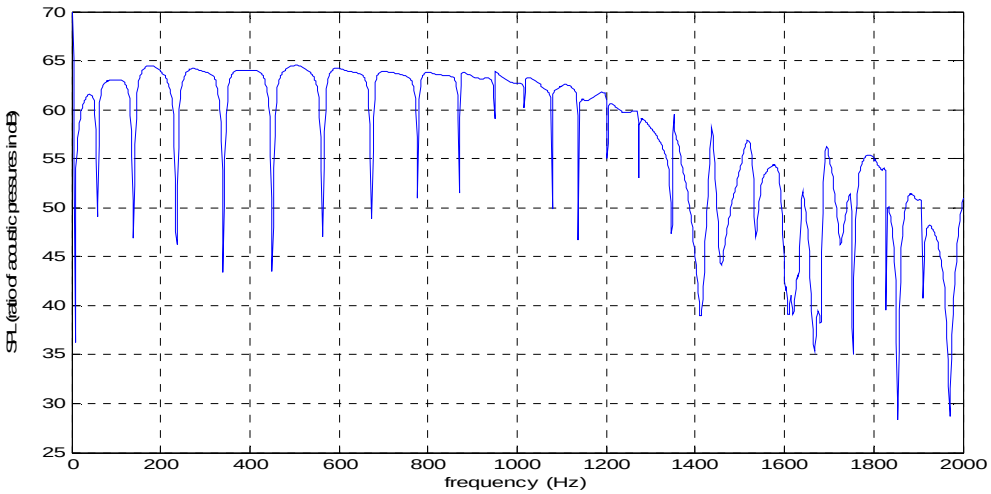

Figure 0-4 SPL values for Regular Honeycomb sandwich panel with Water on Incident & Air on transmitted field

4.6.5 Auxetic honeycomb panel with water on both sides

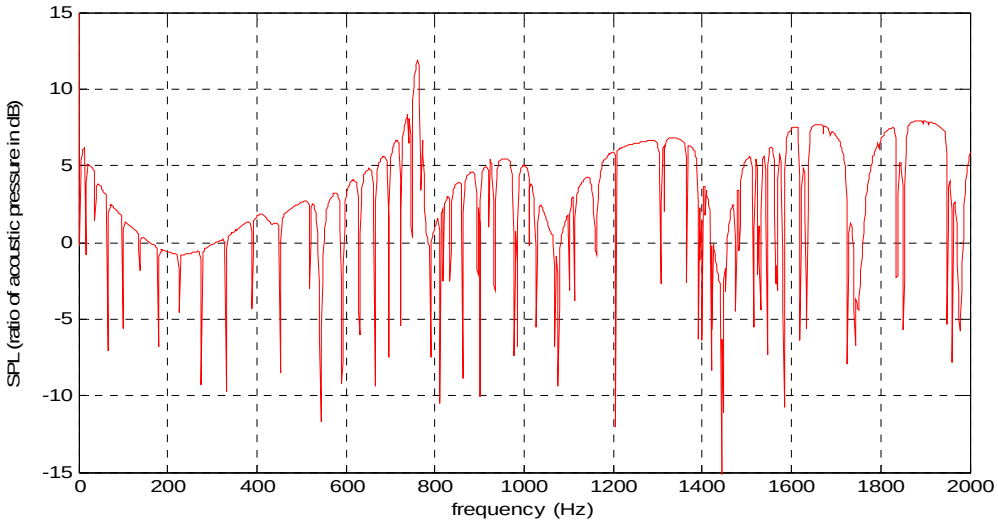

Figure 0-5 SPL values of Auxetic Honeycomb sandwich panel with water on both sides

4.6.6 Water on incident and air on transmitted side

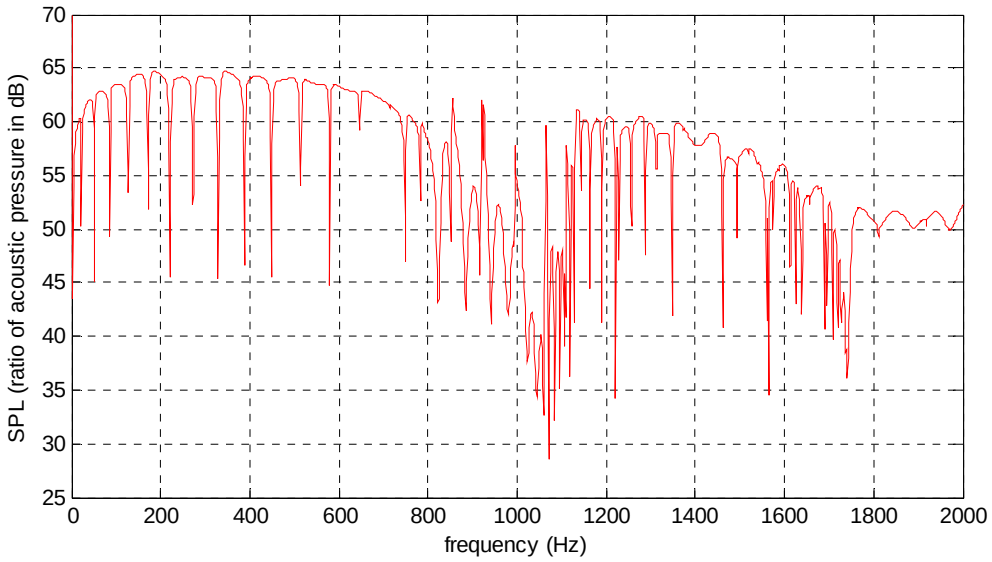

Figure 0-6 SPL values of Auxetic Honeycomb sandwich panel with Water on Incident and Air on Transmitted field

4.6.7 Air on incident side and water on transmitted side

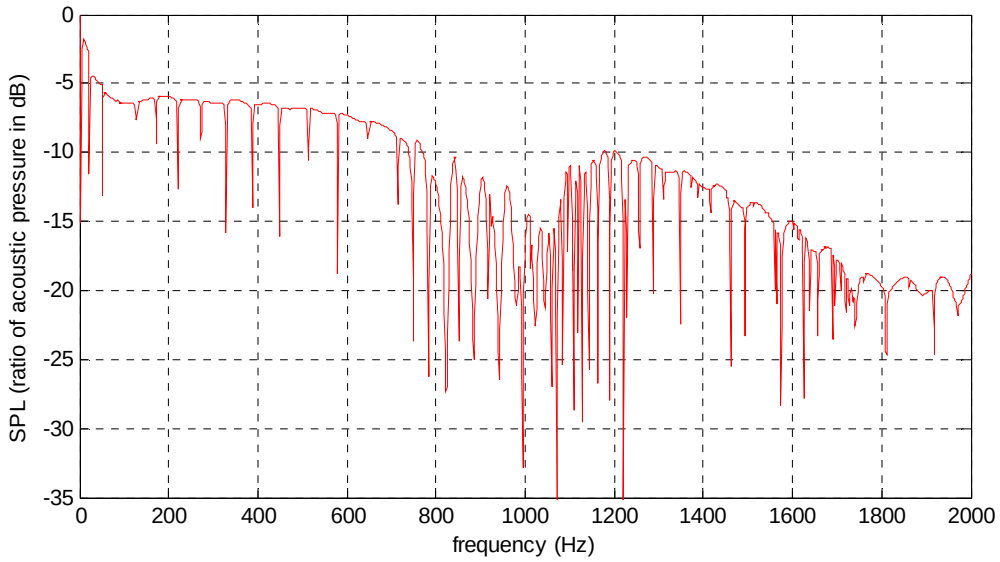

Figure 0-7 SPL values of Auxetic Honeycomb sandwich panel with Air on Incident and Water on Transmitted field

WORKS CITED

[1] Fahy F. and Gardonio P., "6 - Acoustically Induced Vibration of Structures," In: Fahy F. and Gardonio P., editors. Sound and Structural Vibration (Second Edition), Academic Press, Oxford, 2007, 375-401.

[2] London A., "Transmission of reverberant sound through double walls," *J.Acoust.Soc.Am.* **22**(2):270-279, 2005.

[3] Mulholland K., Parbrook H., and Cummings A., "The transmission loss of double panels," *J.Sound Vibrat.* **6**(3):324-334, 1967.

[4] Lin G. and Garrelick J.M., "Sound transmission through periodically framed parallel plates," *J.Acoust.Soc.Am.* **61**(4):1014-1018, 1977.

[5] Wang J., Lu T.J., Woodhouse J., Langley R.S., et al., "Sound transmission through lightweight double-leaf partitions: theoretical modelling," *J.Sound Vibrat.* **286**(4–5):817-847, 2005, doi:http://dx.doi.org/10.1016/j.jsv.2004.10.020.

[6] Brunskog J., "The influence of finite cavities on the sound insulation of double-plate structures," *J.Acoust.Soc.Am.* **117**(6):3727-3739, 2005.

[7] Degischer H.P.and Kriszt B., "Handbook of cellular metals," Wiley-vch, 2002.

[8] Ruzzene M., "Vibration and sound radiation of sandwich beams with honeycomb truss core," *J.Sound Vibrat.* **277**(4):741-763, 2004.

[9] Galgalikar R.R., *Design Automation and Optimization of honeycomb structures for maximum sound transmission loss*, 2012.

[10] Griese D.C., "Finite Element Modeling and Design of Honeycomb Sandwich Panels for Acoustic Performance," *Finite Element Modeling and Design of Honeycomb Sandwich Panels for Acoustic Performance*, 2012.

[11] Rossing T.D., "Springer handbook of acoustics," Springer, 2007.

[12] Denli H. and Sun J., "Structural-acoustic optimization of sandwich structures with cellular cores for minimum sound radiation," *J.Sound Vibrat.* **301**(1):93-105, 2007.

[13] Thamburaj P. and Sun J., "Effect of material anisotropy on the sound and vibration transmission loss of sandwich aircraft structures," *Journal of Sandwich Structures and Materials* **1**(1):76-92, 1999.

[14] Möser M., "Engineering acoustics," *An Introduction to Noise Control.Springter*, 2004.

[15] Thompson L.L. and Huan R., "Computation of far-field solutions based on exact nonreflecting boundary conditions for the time-dependent wave equation," *Comput.Methods Appl.Mech.Eng.* **190**(11):1551-1577, 2000.